







# Bardet–Biedl Syndrome ciliopathy is linked to altered hematopoiesis and dysregulated self-tolerance

Oksana Tsyklauri<sup>1,2,†</sup> , Veronika Niederlova<sup>1,†</sup> , Elizabeth Forsythe<sup>3,4</sup>, Avishek Prasai<sup>1</sup>, Ales Drobek<sup>1</sup> , Petr Kasperek<sup>5,6</sup>, Kathryn Sparks<sup>4</sup>, Zdenek Trachtulec<sup>7</sup>, Jan Prochazka<sup>5,6</sup>, Radislav Sedlacek<sup>5,6</sup>, Philip Beales<sup>3,4</sup> , Martina Huranova<sup>1,\*</sup>  & Ondrej Stepanek<sup>1,\*\*</sup> 

## Abstract

Bardet–Biedl Syndrome (BBS) is a pleiotropic genetic disease caused by the dysfunction of primary cilia. The immune system of patients with ciliopathies has not been investigated. However, there are multiple indications that the impairment of the processes typically associated with cilia may have influence on the hematopoietic compartment and immunity. In this study, we analyze clinical data of BBS patients and corresponding mouse models carrying mutations in *Bbs4* or *Bbs18*. We find that BBS patients have a higher prevalence of certain autoimmune diseases. Both BBS patients and animal models have altered red blood cell and platelet compartments, as well as elevated white blood cell levels. Some of the hematopoietic system alterations are associated with BBS-induced obesity. Moreover, we observe that the development and homeostasis of B cells in mice is regulated by the transport complex BBSome, whose dysfunction is a common cause of BBS. The BBSome limits canonical WNT signaling and increases CXCL12 levels in bone marrow stromal cells. Taken together, our study reveals a connection between a ciliopathy and dysregulated immune and hematopoietic systems.

**Keywords** Bardet–Biedl Syndrome; ciliopathy; CXCL12; immunity; obesity

**Subject Categories** Haematology; Immunology; Molecular Biology of Disease

**DOI** 10.15252/embr.202050785 | Received 30 April 2020 | Revised 4 December 2020 | Accepted 9 December 2020 | Published online 11 January 2021

**EMBO Reports (2021) 22: e50785**

See also: **T Kanie & PK Jackson** (February 2021)

## Introduction

Bardet–Biedl Syndrome (BBS) is a recessive genetic disorder caused by complete or partial loss-of-function mutations in any of 24 genes known to date (*BBS1–23* (Lindstrand *et al*, 2016; Forsythe *et al*, 2018; Wormser *et al*, 2019), *NPHP1* (Lindstrand *et al*, 2014)). BBS belongs to a group of ciliopathies, i.e., disorders caused by defective formation and/or function of primary cilia. Eight BBS proteins (*BBS1*, *BBS2*, *BBS4*, *BBS5*, *BBS7*, *BBS8*, *BBS9*, and *BBS18*) form a transport complex called the BBSome, which sorts selected cargoes into and out of the cilium (Berbari *et al*, 2008; Jin *et al*, 2010; Wei *et al*, 2012; Klink *et al*, 2017). Other commonly mutated BBS genes (*ARL6/BBS3*, *MKKS/BBS6*, *BBS10*, and *BBS12*) assist the assembly or function of the BBSome (Jin *et al*, 2010; Zhang *et al*, 2012a). The BBSome acts as an adaptor connecting ciliary cargoes to intraflagellar transport (IFT) machinery (Liu & Lechtreck, 2018; Ye *et al*, 2018).

Bardet–Biedl Syndrome is a pleiotropic disease whose primary diagnostic features are rod-cone dystrophy, polydactyly, obesity, learning difficulties, hypogonadism, and renal anomalies (Beales *et al*, 1999). The immune system of patients with ciliopathies including BBS has not been studied in detail. An exception in this respect is a case report of three BBS patients suffering from autoimmune diseases in a cohort of 15 studied BBS patients (Halac & Herzog, 2012). The possible connection between ciliopathies and the immune system has not been addressed most likely because immune cells do not form primary cilia (Wheatley *et al*, 1996; Plotnikova *et al*, 2009). However, there are several lines of evidence suggesting that the BBS affects the function of the immune system.

First, the immunological synapse formed between T cells and antigen-presenting cells exhibits a striking analogy to the primary

1 Laboratory of Adaptive Immunity, Institute of Molecular Genetics of the Czech Academy of Sciences, Prague, Czech Republic

2 Faculty of Science, Charles University, Prague, Czech Republic

3 Genetics and Genomic Medicine Programme, University College London Great Ormond Street Institute of Child Health, London, UK

4 National Bardet–Biedl Syndrome Service, Department of Clinical Genetics, Great Ormond Street Hospital, London, UK

5 Laboratory of Transgenic Models of Diseases, Division BIOCEV, Institute of Molecular Genetics of the Czech Academy of Sciences, Vestec, Czech Republic

6 Czech Centre for Phenogenomics, Division BIOCEV, Institute of Molecular Genetics of the Czech Academy of Sciences, Vestec, Czech Republic

7 Laboratory of Germ Cell Development, Division BIOCEV, Institute of Molecular Genetics of the Czech Academy of Sciences, Prague, Czech Republic

\*Corresponding author. Tel: +420 296442256; E-mail: martina.huranova@img.cas.cz

\*\*Corresponding author. Tel: +420 241062155; E-mail: ondrej.stepanek@img.cas.cz

†These authors contributed equally to this work

cilium (Finetti *et al*, 2011; de la Roche *et al*, 2016). The formation of these structures involves the reorganization of cortical actin and the centrosome polarization. In the same vein, some components of the IFT machinery have been shown to participate in the organization of the immunological synapse to promote T-cell activation (Yuan *et al*, 2014; Vivar *et al*, 2016). In particular, it has been shown that vesicles containing key T-cell signaling molecules, the TCR/CD3 complex and LAT, are transported toward the immunological synapse by IFT proteins (Finetti *et al*, 2009; Finetti *et al*, 2014). The BBSome may regulate T-cell activation by transporting signaling proteins into and/or out of the immunological synapse. Depending on the character of these putative cargoes and the direction of the transport, the BBSome could be a positive or a negative regulator of T-cell signaling.

Second, the BBSome is required for Sonic hedgehog (SHH) signaling (Zhang *et al*, 2011; Zhang *et al*, 2012b; Goetz *et al*, 2017). The SHH signaling pathway regulates multiple processes in the organism including T-cell development and differentiation (Shah *et al*, 2004; El Abdaloussi *et al*, 2006; Crompton *et al*, 2007; Rowbotham *et al*, 2008; Drakopoulou *et al*, 2010; Furmanski *et al*, 2013). Key components of the SHH signaling pathway, SMO, IHH, GLI1, and PTCH2, are upregulated in effector cytotoxic T cells and transported toward the immunological synapse in vesicles (de la Roche *et al*, 2013). Moreover, *Smo*<sup>KO/KO</sup> T cells show reduced cytotoxicity associated with defects in the polarized release of cytotoxic granules (de la Roche *et al*, 2013).

Third, the BBSome regulates trafficking of the leptin receptor (Guo *et al*, 2016). Leptin is a signaling molecule which acts as a pro-inflammatory cytokine (Procaccini *et al*, 2012; La Cava, 2017). In particular, leptin signaling inhibits the proliferation of regulatory T cells (De Rosa *et al*, 2007) and promotes the proliferation of effector T cells and their polarization toward Th1 helper cells (Martin-Romero *et al*, 2000). Moreover, T cells deficient in the leptin receptor show impaired differentiation into Th17 helper T cells in mice (Reis *et al*, 2015), indicating a T-cell intrinsic role of leptin signaling.

Fourth, the BBSome tunes WNT signaling by promoting the non-canonical pathway and suppressing the canonical WNT signaling (Ross *et al*, 2005; Gerdes *et al*, 2007). Since WNT signaling is an important regulator of hematopoiesis (Staal *et al*, 2016; Richter *et al*, 2017), the BBSome deficiency might lead to defective formation of blood cells including leukocytes.

Fifth, one of the major symptoms of BBS is obesity, which is believed to undermine the immune tolerance (Johnson *et al*, 2012). Obesity induces production of pro-inflammatory cytokines, such as TNF (Park *et al*, 2005) and IL-6 (Moro *et al*, 2010). These may predispose individuals to the development of autoimmune diseases (Gremese *et al*, 2014; Granata *et al*, 2017; Owczarczyk-Saczonek & Placek, 2017; Singh *et al*, 2017; Wang & He, 2018). Thus, the BBSome may have an extrinsic role in the immune system via inducing obesity.

In this study, we addressed the intrinsic and extrinsic roles of the BBSome in the immune system by investigating BBS patients and mouse models of the BBSome deficiency. We found that BBS patients show elevated prevalence of particular autoimmune diseases. Moreover, our data revealed dysregulated homeostasis of blood cells both in BBS mouse models and in BBS patients.

## Results

### Autoimmune diseases are more prevalent in BBS patients

In this work, we studied the potential role of the BBSome in the immune system. Initially, we analyzed two cohorts of BBS patients from the CRIBBS NIH registry and from the Guy's Hospital of Guy's and St Thomas' NHS Foundation Trust, London, or Great Ormond Street Hospital, London. We found out that certain autoimmune and inflammatory diseases, such as type I diabetes, Hashimoto's thyroiditis, rheumatoid arthritis, and inflammatory bowel diseases, are more prevalent in BBS patients than in the overall population (Table 1). The co-occurrence of multiple autoimmune diseases was relatively small (Appendix Tables S1 and S2). The prevalence of autoimmunity does not seem to be restricted to any causative gene (Appendix Tables S3 and S4). Most frequent causative genes in our cohort were *BBS1* and *BBS10*. Patients with mutations in *BBS10* showed slightly higher prevalence of autoimmunity than patients with mutations in *BBS1*, which is in line with typically higher disease severity in the former group (Niederlova *et al*, 2019). However, the sample size was too small to draw any conclusions. Overall, these findings suggested that the BBSome has an intrinsic or extrinsic role in the immune system, particularly in the immune tolerance.

### BBSome subunit genes are expressed in mouse lymphoid tissues

In the next step, we employed mouse models to study the putative role of the BBSome in the immune and hematopoietic systems in controlled experiments. First, we tested if the BBSome subunits are expressed in murine lymphoid tissues. We detected the expression of all eight BBSome subunits in the spleen, lymph nodes, and isolated T cells on the mRNA level (Fig 1A). The expression levels of *Bbs2*, *Bbs4*, *Bbs9*, and *Bbs18* in the lymphoid tissues were comparable to the brain and the kidney, two organs where the BBSome plays a major role (ODea *et al*, 1996; Davis *et al*, 2007; Keppler-Noreuil *et al*, 2011; Putoux *et al*, 2012). The other four subunits (*Bbs1*, *Bbs5*, *Bbs7*, and *Bbs8*) were expressed in the lymphoid tissues at 10- to 50-fold lower levels than in the brain and the kidney. Moreover, we detected BBS4 protein in isolated T and B cells (Fig 1B). Altogether, all the BBSome subunits are variably expressed in lymphocytes and lymphocyte-rich tissue, despite of the fact that hematopoietic cells are commonly considered as non-ciliated cells. This suggested that the BBSome as a whole or some individual BBSome subunits might have an intrinsic role in lymphocytes.

### Mouse models for studying the role of the BBSome in the immune system

Our next step was to obtain a mouse model of BBS. We decided to use the *Bbs4*-deficient mouse for the following reasons: (i) *BBS4* is an essential part of the BBSome (Klink *et al*, 2017), (ii) *Bbs4*<sup>KO/KO</sup> mouse has been shown to have a relatively severe phenotype in comparison to other BBSome-deficient mice (Rahmouni *et al*, 2008; Guo *et al*, 2011), (iii) *Bbs4* had a relatively high expression in lymphoid tissues (Fig 1A and B). In the following experiments, we used mice with an interrupted *Bbs4* gene with a gene trap (GT allele) cassette, mice with deleted *Bbs4* exon 6 (KO allele), and mice

**Table 1. Autoimmune diseases in BBS patients.**

| CRIBBS registry   |                      |                              |                     |                               |            |          |
|---|----------------------|------------------------------|---------------------|-------------------------------|------------|----------|
|   | Cases/total          | % Prevalence in BBS patients | % Normal prevalence | Fold difference in prevalence | Odds ratio | P-value  |
| Arthritis   | 17/172               | 9.88                         | 0.86                | 11.49                         | 12.64      | 2.73e-13 |
| Type 1 diabetes mellitus  | 6/217                | 2.76                         | 0.48                | 5.76                          | 5.9        | 6.99e-4  |
| Hashimoto's thyroiditis   | 6/235                | 2.55                         | 0.79                | 3.23                          | 3.29       | 0.01     |
| Ulcerative colitis  | 2/255                | 0.78                         | 0.03                | 26.14                         | 26.34      | 2.77e-3  |
| Celiac disease  | 2/255                | 0.78                         | 0.75                | 1.05                          | 1.05       | 0.72     |
| At least one autoimmune condition CRIBBS  | 29 <sup>a</sup> /255 | 11.37                        | 4.93                | 2.31                          | 2.47       | 3.16e-5  |
| Great Ormond Street Hospital & Guy's Hospital cohort  |                      |                              |                     |                               |            |          |
|   | Cases/total          | % Prevalence in BBS patients | % Normal prevalence | Fold change prevalence        | Odds ratio | P-value  |
| Hypothyroidism  | 22/198               | 11.11                        | 5.30                | 2.10                          | 2.23       | 1.15e-3  |
| Celiac disease  | 4/198                | 2.02                         | 0.75                | 2.69                          | 2.73       | 0.06     |
| Inflammatory bowel diseases   | 3/198                | 1.51                         | 0.40                | 3.79                          | 3.83       | 0.05     |
| Type 1 diabetes mellitus  | 3/198                | 1.51                         | 0.48                | 3.16                          | 3.19       | 0.07     |
| Psoriasis   | 2/198                | 1.01                         | 0.20                | 5.05                          | 5.09       | 0.06     |
| Other diseases with one occurrence (Immune thrombocytopenic purpura, Henoch-Schönlein purpura, Sarcoidosis, Vitiligo) | 4/198                |                              |                     |                               |            |          |
| At least one autoimmune condition UK  | 33 <sup>b</sup> /198 | 16.67                        | 4.93                | 3.38                          | 3.86       | 9.76e-10 |

The table shows the fold difference in the prevalence (prevalence in BBS patients/general prevalence) and the odds ratio of autoimmune diseases in the CRIBBS cohort of 255 BBS patients (upper part) and in the cohort of 198 BBS patients from Great Ormond Street Hospital and Guy's Hospital in London (lower part). Normal prevalence of autoimmune diseases was adopted from (Hayter & Cook, 2012; Martel-Pelletier et al, 2016; Taylor et al, 2018). Statistical significance was calculated using exact binomial test.

<sup>a</sup>Total count is not equal to sum of all the patients with autoimmune diseases because of the co-occurrence of more than one disease in 4 patients. Co-occurring diseases are listed in Appendix Table S1.

<sup>b</sup>Total count is not equal to sum of all the patients with autoimmune diseases because of the co-occurrence of more than one disease in 5 patients. Co-occurring diseases are listed in Appendix Table S2.

with *Bbs4* exon 6 flanked with LoxP sites (FL allele) enabling the conditional deletion of this exon (cKO; Fig 1C).

BBS4 protein was not detectable in the testes, thymi and brain from the *Bbs4*<sup>GT/GT</sup> mice (Fig 1D and E). As expected, the *Bbs4* deficiency lead to the absence of sperm flagella in testes of 30-days-old *Bbs4*<sup>GT/GT</sup> males (Fig 1F). However, we did not observe two previously reported features of BBS mouse models in *Bbs4*<sup>GT/GT</sup> mice. Although mating of *Bbs4*<sup>+/GT</sup> heterozygotes resulted to 17% *Bbs4*<sup>GT/GT</sup> pups at weaning, only 2% *Bbs4*<sup>KO/KO</sup> pups were produced in mating of *Bbs4*<sup>+/KO</sup> heterozygotes (Fig 1G). This suggests that *Bbs4*<sup>KO/KO</sup>, but not *Bbs4*<sup>GT/GT</sup>, mice suffer from frequent pre-weaning lethality. Moreover, *Bbs4*<sup>KO/KO</sup> mice, but not *Bbs4*<sup>GT/GT</sup>, developed obesity (Fig 1H–J). As expected, adult *Bbs4*<sup>KO/KO</sup> mice, suffering from obesity, had elevated levels of leptin in blood plasma in comparison to non-obese *Bbs4*<sup>GT/GT</sup> mice, and pre-obese young *Bbs4*<sup>KO/KO</sup> mice (Fig 1K). Because leptin has been proposed to act as a pro-inflammatory molecule, it might have an impact on the immune system of obese BBS mice.

To explain the phenotypic difference between *Bbs4*<sup>GT/GT</sup> and *Bbs4*<sup>KO/KO</sup> mice, we analyzed the respective *Bbs4* transcripts via RT-PCR. Although transcript of *Bbs4*<sup>KO</sup> allele lacked the exon 6 as expected, we detected a transcript containing all exons 5–11 in *Bbs4*<sup>GT/GT</sup> mice (Fig EV1A). Unexpectedly, the RNA polymerase II is

able to read through two transcription termination sites in the gene trap cassette in *Bbs4*<sup>GT/GT</sup> tissues to generate *Bbs4* mRNA at ~ 10% of the wild-type (WT) levels (Fig EV1B). However, the PCR product of *Bbs4*<sup>GT</sup> mRNA was longer than the respective amplicon of the WT allele (Fig EV1A and B). Sequencing revealed that *Bbs4*<sup>GT</sup> allele is mis-spliced and includes a short insert originating from the gene trap cassette, which induces a frame shift in the open reading frame (Fig EV1C). Expression of this *Bbs4*<sup>GT</sup> cDNA in HEK293T cells resulted in a very tiny production of truncated BBS4 (Fig EV1D), possibly via an alternative transcription/translation start. It is plausible that low levels of this truncated BBS4 are present in *Bbs4*<sup>GT/GT</sup> tissues as well. Moreover, we could detect a small amount (~ 1% of WT levels) of properly spliced *Bbs4* mRNA in *Bbs4*<sup>GT/GT</sup> brain (Fig EV1E). Overall, these data indicate that *Bbs4*<sup>KO</sup> is a null allele, whereas *Bbs4*<sup>GT</sup> is a hypomorphic allele.

#### Altered B-cell compartment in *Bbs4* deficient mice

To analyze the role of the BBSome in the formation of adaptive immune cells, we analyzed the development and homeostasis of T and B cells in *Bbs4*-deficient mice. We did not observe any major alterations in the T-cell compartment in *Bbs4*<sup>KO/KO</sup> and *Bbs4*<sup>GT/GT</sup> mice (Fig EV2A–F). The only significant differences were decreased

percentage of T cells among the splenocytes (Fig EV2C) and decreased percentage of CD44<sup>+</sup> cells among splenic CD8<sup>+</sup> T cells of the *Bbs4*<sup>KO/KO</sup> mice (Fig EV2F).

We found an alteration of the B-cell development and/or homeostasis in *Bbs4*-deficient mice. The total numbers of bone marrow B220<sup>+</sup> B-cell lineage cells were not significantly altered in *Bbs4*<sup>KO/KO</sup>

or *Bbs4*<sup>GT/GT</sup> mice (Fig EV3A). However, the ratio of B220<sup>high</sup> and B220<sup>low</sup> cells in the bone marrow was shifted toward less mature B220<sup>low</sup> cells in *Bbs4*<sup>KO/KO</sup> mice and, to a lesser extent, in *Bbs4*<sup>GT/GT</sup> mice (Fig 2A). Both *Bbs4*<sup>KO/KO</sup> and *Bbs4*<sup>GT/GT</sup> mice had higher percentage of IgD<sup>-</sup> IgM<sup>-</sup> B-cell precursors than controls (Fig 2B). A deeper analysis of this population showed that *Bbs4*-deficiency

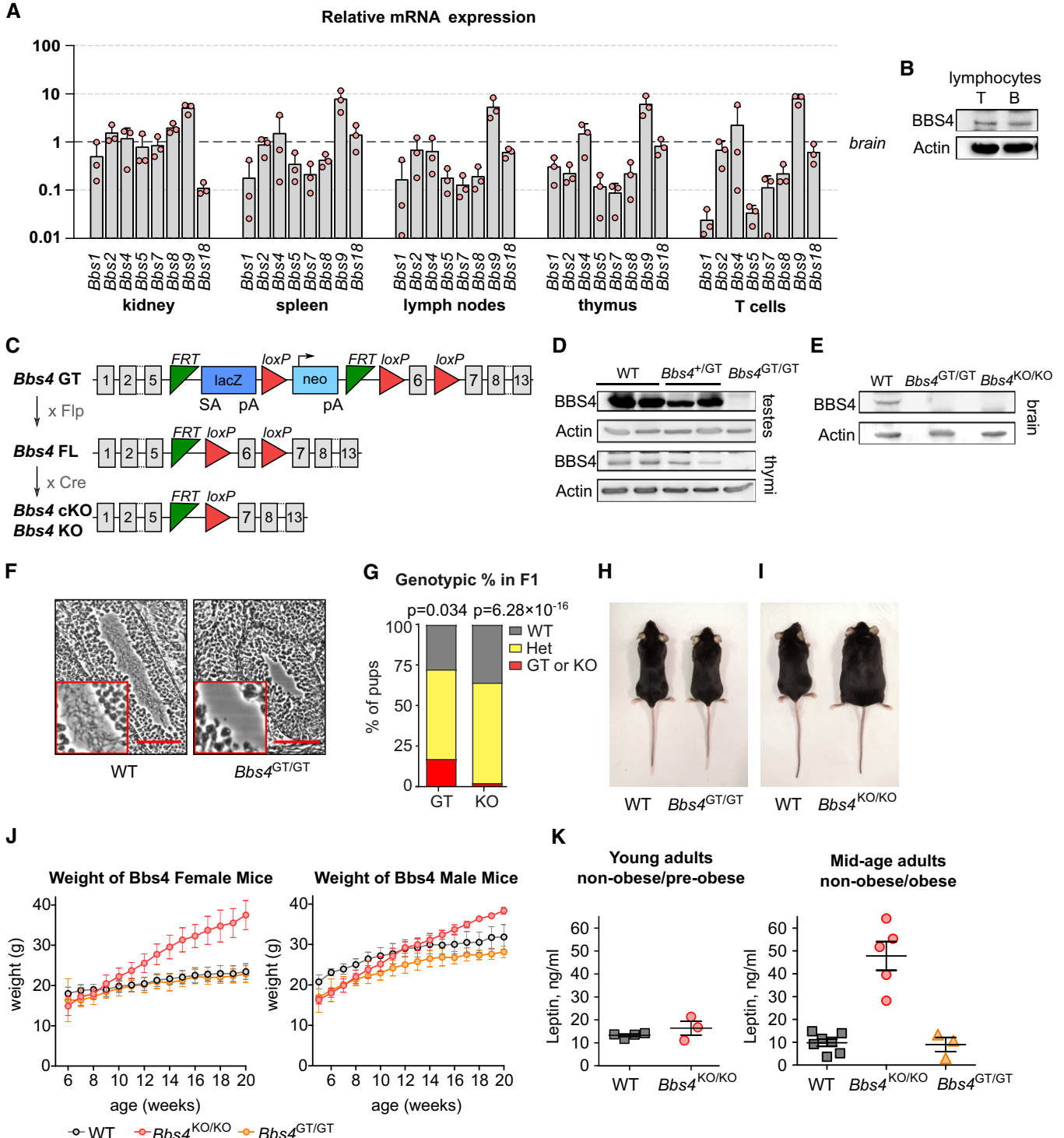


Figure 1.

**Figure 1. Basic characterization of *Bbs4*-deficient mouse models.**

- A Relative expression of the BBSome subunits in the indicated organs and T cells measured by qPCR.  $C_T$  values of the BBS genes were normalized to the geometric mean of the  $C_T$  values of reference genes *Gapdh*, *Tubb2a*, and *Eef1a1*. The expression levels are normalized to those of brain (= 1). Mean + SD. Three biological replicates (the result of each biological replicate is a median of three technical replicates).
- B Immunoblot analysis of BBS4 expression in T and B lymphocytes isolated from the lymph nodes and spleen of C57Bl/6 mouse.  $\beta$ -actin staining served as a loading control. The identical immunoblot is shown in Fig EV4A. A representative experiment out of three biological replicates in total is shown.
- C Schematic representation of mouse models of *Bbs4* deficiency used in this study. *Bbs4* GT, gene trap allele interrupting the *Bbs4* gene. *Bbs4* FL, allele with floxed *Bbs4* exon 6. *Bbs4* KO and cKO alleles with deleted exon 6.
- D Immunoblot analysis of BBS4 expression in testes and thymi lysates of *Bbs4*<sup>+/+</sup> (WT), *Bbs4*<sup>GT/+</sup>, and *Bbs4*<sup>GT/GT</sup> mice.  $\beta$ -actin staining serves as a loading control. A representative experiment out of three biological replicates in total is shown.
- E Immunoblot analysis of BBS4 expression in the brain lysates of *Bbs4*<sup>+/+</sup>, *Bbs4*<sup>GT/GT</sup>, and *Bbs4*<sup>KO/KO</sup> mice.  $\beta$ -actin staining served as a loading control. A representative experiment out of two biological replicates is shown.
- F Hematoxylin and eosin staining of sections of seminiferous tubules from ~ 4 weeks old *Bbs4*<sup>+/+</sup> ( $n = 2$  mice) and *Bbs4*<sup>GT/GT</sup> ( $n = 4$ ) males. Scale bar, 100  $\mu$ m. Representative images are shown.
- G Genotypic ratio of *Bbs4*<sup>+/+</sup>, *Bbs4*<sup>GT/+</sup> or *Bbs4*<sup>KO/+</sup> (Het), and *Bbs4*<sup>GT/GT</sup> (GT) or *Bbs4*<sup>KO/KO</sup> (KO) offspring at weaning from mating of *Bbs4*<sup>GT/+</sup> ( $n = 145$  pups) or *Bbs4*<sup>+/KO</sup> ( $n = 168$  pups) parents. Binomial test was used for statistical comparison of the observed distribution to the expected Mendelian ratio.
- H *Bbs4*<sup>+/+</sup> and *Bbs4*<sup>GT/GT</sup> female littermates at 20 weeks of age. Representative litter out of seven in total.
- I *Bbs4*<sup>+/+</sup> and *Bbs4*<sup>KO/KO</sup> female littermates at 20 weeks of age. Representative litter out of five in total.
- J Growth curves of *Bbs4*-deficient mice, mean  $\pm$  SD is shown. Females: *Bbs4*<sup>+/+</sup> ( $n = 12$  mice), *Bbs4*<sup>GT/GT</sup> ( $n = 12$ ), *Bbs4*<sup>KO/KO</sup> ( $n = 6$ ). Males: *Bbs4*<sup>+/+</sup> ( $n = 6$  mice), *Bbs4*<sup>GT/GT</sup> ( $n = 7$ ), *Bbs4*<sup>KO/KO</sup> ( $n = 5$ ).
- K Leptin concentration in blood plasma taken from young adult (7–8 weeks) or mid-age (14–20 weeks) mice. Young adult mice: *Bbs4*<sup>+/+</sup> ( $n = 4$  mice), *Bbs4*<sup>KO/KO</sup> ( $n = 3$ ), analyzed in two independent experiments. Mid-age adult mice: *Bbs4*<sup>+/+</sup> ( $n = 7$  mice), *Bbs4*<sup>KO/KO</sup> ( $n = 5$ ), *Bbs4*<sup>GT/GT</sup> ( $n = 3$ ), analyzed in 4 independent experiments. Kruskal–Wallis tests were used for the statistical analysis. Mean  $\pm$  SEM.

Source data are available online for this figure.

results in the accumulation of pre-B cells, which is the developmental stage when the pre-B-cell receptor selection occurs (Fig 2C).

We observed slightly increased numbers of B cells in the spleen of *Bbs4*<sup>KO/KO</sup>, but not *Bbs4*<sup>GT/GT</sup> mice (Fig EV3B and C). In the spleen and lymph nodes, *Bbs4*<sup>KO/KO</sup> and *Bbs4*<sup>GT/GT</sup> mice showed larger late mature B-cell population (IgD<sup>+</sup> IgM<sup>-</sup>) than WT mice (Figs 2D and E, and EV3D and E). In addition, *Bbs4*<sup>KO/KO</sup> showed ~ 2-fold lower percentage of splenic marginal zone (MZ) B cells (Fig 2F).

To address whether the phenotype of *Bbs4*<sup>KO/KO</sup> is indeed caused by the BBSome dysfunction, we generated a second mouse model of BBS based on the genetic disruption of another BBSome subunit, BBS18 (alias BBIP1; Fig EV3F). Unfortunately, we observed strong pre-weaning lethality resulting in only two adult *Bbs18*<sup>KO/KO</sup> animals overall (Fig EV3G). The comparison of these *Bbs18*<sup>KO/KO</sup> animals to their WT and *Bbs18*<sup>+/KO</sup> littermates showed very similar phenotype to *Bbs4*<sup>KO/KO</sup> mice, i.e., increased B-cell precursors in the bone marrow (Fig EV3H) and decreased MZ B cells in the spleen (Fig EV3I). These data indicated that the alterations of the B-cell lineage are not unique to the deficiency in BBS4, but are likely a common feature of the BBSome disruption.

Overall, these data show that BBSome deficiency results in an abnormal development of B cells in the bone marrow, a slightly increased percentage of late mature splenic B cells and a reduction of splenic MZ B cells in the periphery. The developmental alteration was observed also in non-obese *Bbs4*<sup>GT/GT</sup> mice, indicating that this phenotype is largely obesity-independent.

### ***Bbs4* deficiency does not intrinsically influence antigen-specific T-cell and B-cell responses**

As we observed an alteration of B-cell homeostasis in *Bbs4*-deficient mice, we decided to investigate how it affects the response of the adaptive immune system. First, we activated monoclonal B cells specific for 4-hydroxy-3-nitrophenyl acetyl (NP) from B-cell receptor transgenic B1–8 mice (Sonoda *et al*, 1997) and *Bbs4*<sup>GT/GT</sup> B1–8 mice

using NP-labeled cells. In this setup, we monitored the upregulation of the activation marker CD69 (Fig 3A and B). Moreover, we stimulated B cells from *Bbs4*<sup>KO/KO</sup>, *Bbs4*<sup>+/KO</sup>, and *Bbs4*<sup>+/+</sup> mice with plate bound anti-IgM antibody (Fig 3C). In these assays, we did not observe any role of *Bbs4* deficiency in the antigenic B-cell response.

Based on the homology between the cilium and the immunological synapse (Finetti *et al*, 2009; Finetti *et al*, 2011; Stephen *et al*, 2018), we hypothesized that the BBSome might act as a positive or negative regulator of T-cell responses. For this reason, we generated *Bbs4*<sup>FL/FL</sup> *Cd4-Cre* mouse line where *Bbs4* deficiency was restricted to T cells (Fig EV4A). These mice did not show any obvious phenotype in the T-cell compartment (Fig EV4B–E). To study the role of the BBSome in T-cell antigenic responses, we crossed *Bbs4*<sup>FL/FL</sup> *Cd4-Cre* mice to TCR transgenic OT-I *Rag2*<sup>KO/KO</sup> mice. This mouse generates monoclonal T cells specific for K<sup>b</sup>-OVA, a model antigen originating from chicken ovalbumin. We did not observe any role of BBS4 in the conjugation of OT-I T cells with antigen-presenting cells loaded with OVA or its lower affinity variants (Fig 3D). Moreover, WT and *Bbs4*-deficient OT-I T cells showed the same ability to induce autoimmune diabetes upon a transfer into RIP.OVA mice expressing ovalbumin under the rat insulin promoter and subsequent priming by *Listeria monocytogenes* expressing ovalbumin (King *et al*, 2012; Palmer *et al*, 2016) (Fig 3E and F). This assay examines T cells for their ability to get primed by the OVA-antigen, expand, infiltrate the pancreas, and kill the  $\beta$ -cells. As the onset of diabetes caused by *Bbs4*-deficient OT-I T cells was not different from the control, we concluded that BBS4 does not play an important intrinsic role in any of indicated steps of the T-cell-mediated immune response.

### **The role of BBS4 in B-cell homeostasis is not intrinsic**

To investigate if the observed B-cell developmental changes in *Bbs4*-deficient mice are B-cell intrinsic, we generated *Bbs4*<sup>FL/FL</sup> *Vav-iCre* mice with a specific deletion of *Bbs4* in the hematopoietic and

endothelial cells (Georgiades *et al*, 2002). We did not observe any evidence of altered B-cell homeostasis in *Vav-iCre* mice (Fig 4A–C). These results suggest that the B-cell compartment in *Bbs4*<sup>GT/GT</sup> and *Bbs4*<sup>KO/KO</sup> mice is affected by factors extrinsic to the hematopoietic lineage.

The development of B cells is guided by the cytokine environment in the bone marrow niche with prominent roles of IL-7 and CXCL12 (Zehentmeier & Pereira, 2019). We observed that the expression of *Cxcl12*, but not *Il-7*, is decreased in the bone marrow of *Bbs4* and *Bbs18* KO mice (Fig 4E). In the next step, we generated

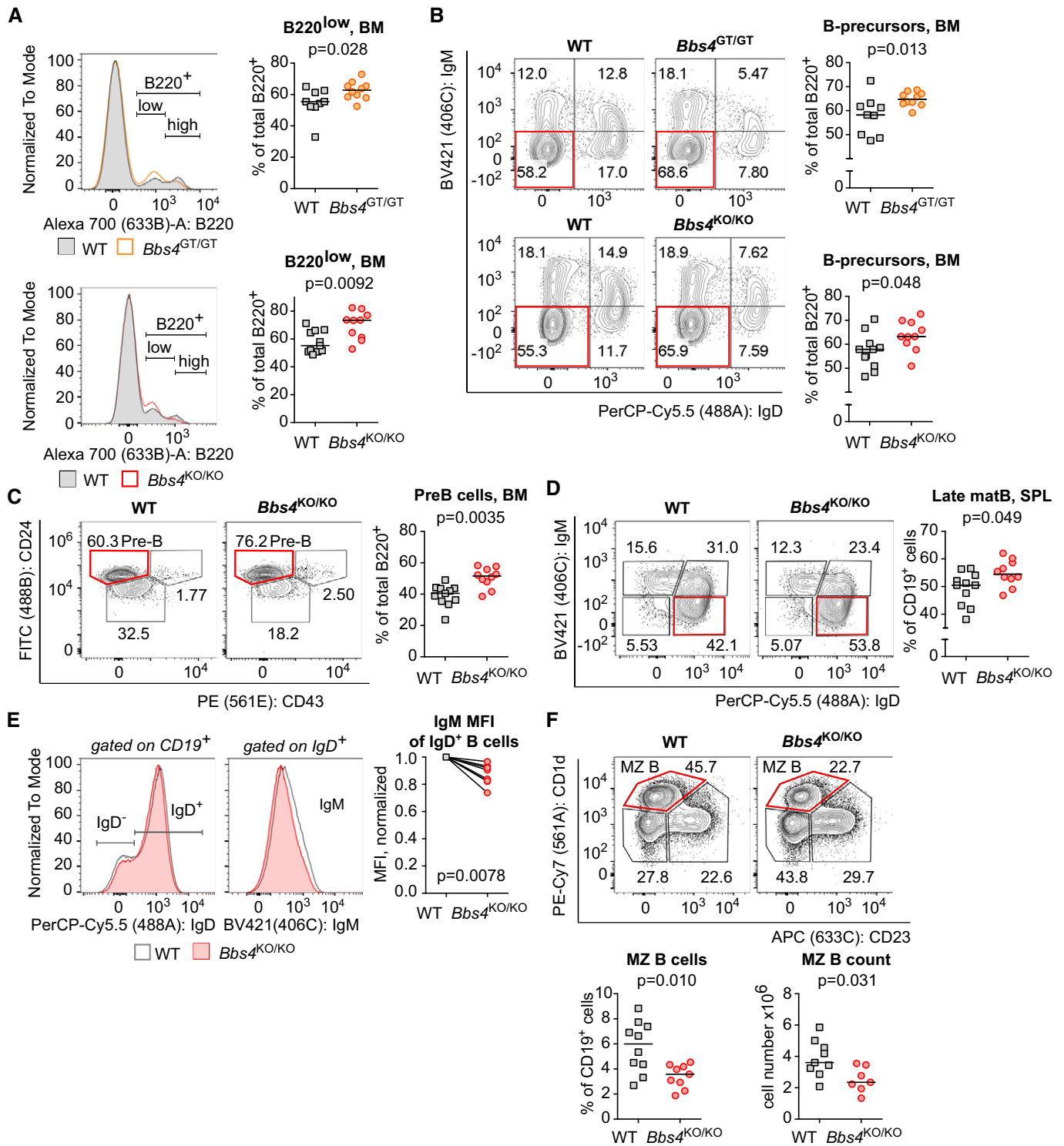


Figure 2.

**Figure 2. B-cell compartment is moderately affected in *Bbs4*-deficient mice.**

Cells isolated from the bone marrow (BM) (A–C) and spleens (SPL) (D–F) of 18- to 25-week-old *Bbs4*<sup>+/+</sup> (WT), *Bbs4*<sup>GT/GT</sup>, and *Bbs4*<sup>KO/KO</sup> mice were analyzed by flow cytometry. Number of analyzed mice (*n*) is indicated. Six (*Bbs4*<sup>GT/GT</sup> strain and *Bbs4*<sup>+/+</sup> controls) or eight (*Bbs4*<sup>KO/KO</sup> strain and *Bbs4*<sup>+/+</sup> controls) independent experiments were performed.

- A Percentage of B220<sup>low</sup> positive cells in the bone marrow. Up: *Bbs4*<sup>+/+</sup> *n* = 9, *Bbs4*<sup>GT/GT</sup> *n* = 10. Down: *Bbs4*<sup>+/+</sup> (*n* = 11), *Bbs4*<sup>KO/KO</sup> (*n* = 10). Statistical significance was calculated using two-tailed Mann–Whitney test. Medians are shown.
- B Percentage of B-cell precursors (IgM<sup>−</sup> IgD<sup>−</sup>) in the bone marrow. Gated on viable B220<sup>+</sup> cells. Up: *Bbs4*<sup>+/+</sup> (*n* = 9), *Bbs4*<sup>GT/GT</sup> (*n* = 10). Down: *Bbs4*<sup>+/+</sup> (*n* = 11), *Bbs4*<sup>KO/KO</sup> (*n* = 10). Statistical significance was calculated using two-tailed Mann–Whitney test. Medians are shown.
- C Percentage of pre-B cells (CD43<sup>−</sup> CD24<sup>high</sup>) in the bone marrow of *Bbs4*<sup>+/+</sup> (*n* = 11) and *Bbs4*<sup>KO/KO</sup> mice (*n* = 10). Gated on viable B220<sup>+</sup> IgM<sup>−</sup> IgD<sup>−</sup> cells. Statistical significance was calculated using two-tailed Mann–Whitney test. Medians are shown.
- D Percentage of late mature (IgM<sup>−</sup> IgD<sup>+</sup>) B cells in the spleen of *Bbs4*<sup>+/+</sup> (*n* = 11) and *Bbs4*<sup>KO/KO</sup> mice (*n* = 10) Gated on viable CD19<sup>+</sup> cells. Statistical significance was calculated using two-tailed Mann–Whitney test. Medians are shown.
- E An alternative analysis of the experiment shown in (D). Geometric mean fluorescence intensity (MFI) of BV421 (IgM) on IgD<sup>+</sup> B cells was determined. Mean of MFI values for each genotype per experiment was quantified, and obtained values were normalized to *Bbs4*<sup>+/+</sup> (= 1) for each experiment. Two-tailed one sample Wilcoxon signed rank test was used for the statistical analysis.
- F Percentage of splenic marginal zone (MZ) B cells (CD23<sup>−</sup> CD1d<sup>+</sup>) in *Bbs4*<sup>+/+</sup> controls (*n* = 10) and *Bbs4*<sup>KO/KO</sup> mice (*n* = 9) was determined. Gated on viable CD19<sup>+</sup>, IgD<sup>−</sup> IgM<sup>+</sup>, CD138<sup>−</sup> cells. Statistical significance was calculated using two-tailed Mann–Whitney test. Medians are shown.

Source data are available online for this figure.

mouse embryonic fibroblasts (MEF) from *Bbs4*<sup>+/+</sup> and *Bbs4*<sup>KO/KO</sup> mice. *Bbs4*<sup>KO/KO</sup> MEFs showed lower expression of *Cxcl12* than *Bbs4*<sup>+/+</sup> MEFs (Fig 4F), indicating that the BBSome regulates *Cxcl12* expression in mesenchymal cells. It has been shown previously that the BBSome inhibits canonical WNT signaling in vertebrates (Gerdes *et al*, 2007) and that the canonical WNT signaling downregulates *Cxcl12* expression in bone marrow stroma-derived ST2 cells (Tamura *et al*, 2011). Accordingly, canonical WNT signaling (triggered by WNT3A), but not non-canonical WNT signaling (triggered by WNT5A), suppressed *Cxcl12* expression in ST2 cells and induced the expression of canonical WNT responsive gene *Alpl* (Fig 4G). We produced *Bbs4*-deficient ST2 cells using CRISPR/Cas9 (Fig EV5A, Appendix Table S6). Two out of four *Bbs4*<sup>KO/KO</sup> ST2 cell clones showed significantly reduced expression of *Cxcl12* (Fig EV5B). Overall, our data indicate that the BBSome deficiency amplifies canonical WNT signaling in bone marrow stromal cells leading to decreased production of CXCL12 and subsequent partial defects in B-cell development.

### BBS-induced obesity affects blood homeostasis

To investigate the possible factors predisposing BBS patients to the development of autoimmune diseases, we examined the blood test results of BBS patients. Intriguingly, immunity-related parameters, such as counts of total white blood cells, neutrophils, and eosinophils, were increased in BBS patients, when compared to age and gender-matched controls (BMI-random controls) (Fig 5A). To address the role of obesity in BBS patients, we used an additional set of controls with body mass indexes (BMI) matching to those of BBS patients (BMI-matched controls). We did not observe any difference when we compared the indicated leukocyte parameters between BBS patients and BMI-matched controls.

We analyzed the peripheral blood of *Bbs4*-deficient mice to further explore the role of the BBSome and the potential involvement of obesity in blood cell homeostasis. In agreement with the analysis of the patients' blood tests, we did not observe major differences between WT and non-obese *Bbs4*<sup>GT/GT</sup> mice. However, obese *Bbs4*<sup>KO/KO</sup> mice showed higher total white blood cell count than WT controls (Fig 5B), which corresponded with the data from patients as well (Fig 5A). These results indicate that obesity in BBS

patients and in *Bbs4*-deficient mice has an impact on the leukocyte homeostasis.

We found that elevated C-reactive protein (CRP) was more frequent in BBS patients than in BMI-matched and BMI-random controls (Fig 5C), which indicates that obesity is not the only factor influencing the immune system of BBS patients. Notably, the homeostasis of red blood cells was altered in BBS patients as well as in the *Bbs4*<sup>KO/KO</sup> mice, although at different levels (Fig 5D and E). BBS patients showed low overall hemoglobin levels caused by a mild decrease in the red blood cell count and low red blood cell hemoglobin (Fig 5D), indicating a possibility of a reduced oxygen transport capacity. Interestingly, the comparison of BBS patients with BMI-matched controls showed that the alteration of the erythroid compartment was not caused by obesity. The mouse model of BBS showed a decreased number of red blood cells, which was compensated by enlarged red blood cell volume (Fig 5E).

In addition, we observed decreased platelet counts both in BBS patients and *Bbs4*<sup>KO/KO</sup> mice (Fig 5F–G). The reduction of platelets in BBS patients was not obesity-dependent. Furthermore, *Bbs4*<sup>KO/KO</sup> mice showed higher mean platelet volume and lower plateletcrit than WT mice (Fig 5F–G), indicating enhanced removal of platelets in the periphery.

Altogether, our results suggest a role of the BBSome in the immune tolerance, hematopoiesis and/or blood homeostasis. Most of the effects seem to be extrinsic to the hematopoietic compartment as revealed by using tissue-specific knock-out mouse model and comparison of patients to BMI-matched controls. However, altered CRP levels, red blood cell, and platelet homeostasis in BBS patients are obesity-independent.

## Discussion

In this study we focused on the putative connection between BBS and immune/hematopoietic defects. At first, we hypothesized that the immune system of BBS patients might be substantially influenced by obesity, which is a typical BBS symptom. Obesity can induce the state of low-grade metabolic inflammation characterized by elevated TNF $\alpha$ , IL-6, and CRP in blood (Visser *et al*, 1999;

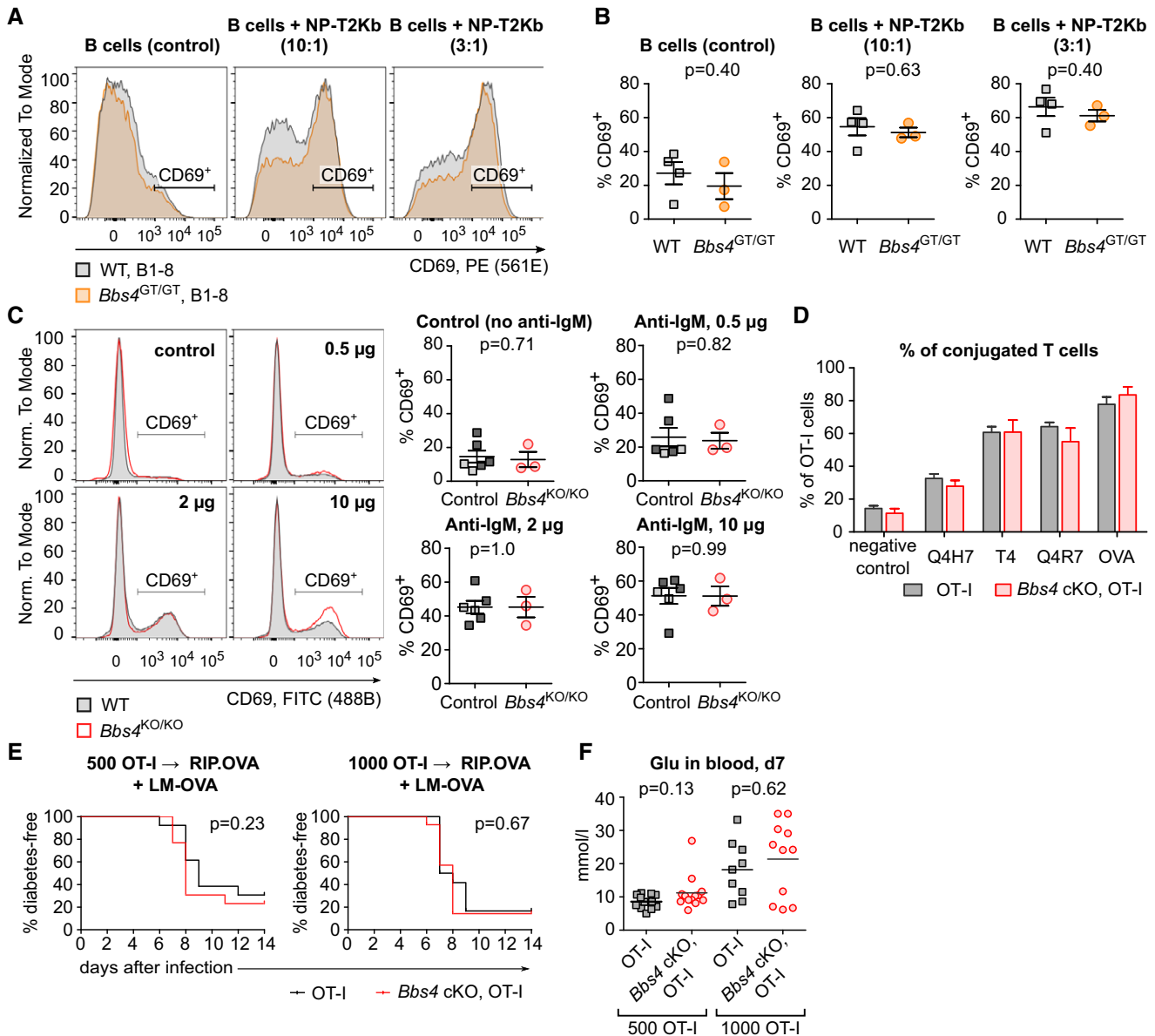


**Figure 3. BBS4 is not required for T-cell and B-cell antigenic responses.**

A, B Splenocytes isolated from *Bbs4*<sup>+/+</sup> ( $n = 4$  mice) and *Bbs4*<sup>GT/GT</sup> ( $n = 3$ ) B-cell transgenic B1–8 littermates were activated with 4-hydroxy-3-nitrophenylacetic acid succinimide ester-loaded T2-Kb cells in three independent experiments. Percentage of activated B cells (gated as CD69<sup>+</sup> B220<sup>+</sup> IgLλ<sup>+</sup> viable cells) in the samples without T2-Kb (negative control), and in the samples with T2-Kb added in ratios 1:10 or 1:3 was determined by flow cytometry. (A) Representative mice are shown. (B) Mean ± SEM. Statistical significance was calculated using two-tailed Mann–Whitney test.

C B cells from 18- to 20-week-old *Bbs4*<sup>KO/KO</sup> (red circle,  $n = 3$  mice), and control mice (*Bbs4*<sup>+/+</sup>, dark gray square,  $n = 4$ , or *Bbs4*<sup>+/KO</sup>, light gray square,  $n = 2$ ) were activated with F(ab')<sub>2</sub>-goat anti-mouse IgM (Mu chain). Percentage of activated B cells (gated as CD69<sup>+</sup> CD19<sup>+</sup> viable cells) was determined by flow cytometry. Representative experiment out of three biological replicates is shown. Mean ± SEM. Statistical significance was calculated using two-tailed Mann–Whitney test.

D CFSE-loaded T cells isolated from lymph nodes of *Bbs4*<sup>FL/FL</sup> OT-I *Rag2*<sup>KO/KO</sup> (OT-I) and *CD4-Cre Bbs4*<sup>FL/FL</sup> OT-I *Rag2*<sup>KO/KO</sup> (*Bbs4* cKO, OT-I) littermates were incubated with DDAO-labeled WT splenocytes loaded with OVA peptide or with the indicated altered peptide ligands for 20 min. Percentage of T cells conjugated with the APCs was determined by flow cytometry. Four biological replicates were performed. Mean + SEM. Statistical significance was calculated using two-tailed Mann–Whitney test,  $P > 0.05$  for all peptides.

E, F 500 or 1,000 T cells isolated from lymph nodes of *Bbs4*<sup>FL/FL</sup> OT-I *Rag2*<sup>KO/KO</sup> (OT-I) and *CD4-Cre Bbs4*<sup>FL/FL</sup> OT-I *Rag2*<sup>KO/KO</sup> (*Bbs4* cKO, OT-I) littermates were adoptively transferred into RIP.OVA mice followed by infection with *Listeria monocytogenes* expressing ovalbumin (LM-OVA) on the next day. (E) Glucose level in the urine of mice was monitored on a daily basis. The mouse was considered diabetic when it had urine glucose level ≥ 1,000 mg/dl for two consecutive days. Statistical significance was calculated by Log-rank (Mantel-Cox) test. (F) Glucose concentration in blood on day 7 post-infection. 500 OT-I ctrl ( $n = 13$  mice), 500 OT-I *Bbs4* cKO ( $n = 13$ ), 1,000 OT-I ctrl ( $n = 9$ ), 1,000 OT-I *Bbs4* cKO ( $n = 11$ ), analyzed in four independent experiments, mean is shown. Statistical significance was calculated using two-tailed Mann–Whitney test.

Source data are available online for this figure.



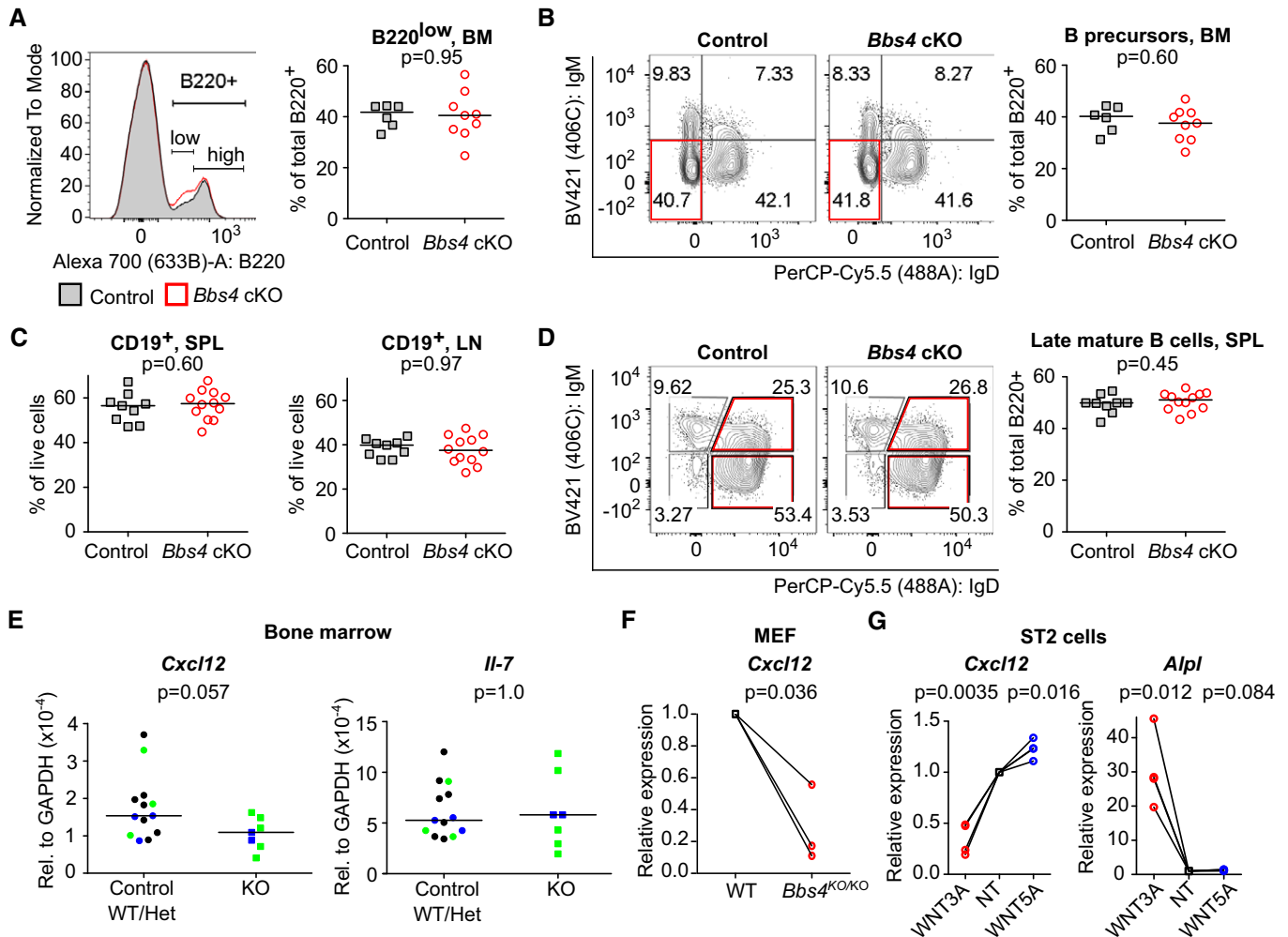


**Figure 4. The role of *Bbs4* in B-cell development is not intrinsic.**

A–D Cells isolated from bone marrow (BM) (A, B), lymph nodes (LN) and spleen (SPL) (C, D) of *Bbs4*<sup>FL/FL</sup> (control) and *Vav-iCre Bbs4*<sup>FL/FL</sup> (cKO) mice were analyzed by flow cytometry. (A) Percentage of B220<sup>low</sup> in bone marrow. Representative experiment out of four in total is shown. *Bbs4*<sup>FL/FL</sup> ( $n = 6$  mice), *Vav-iCre Bbs4*<sup>FL/FL</sup> ( $n = 9$ ). (B) Percentage of B-cell precursors (B220<sup>+</sup>, IgM<sup>-</sup> IgD<sup>-</sup>) in the bone marrow. Representative experiment out of four in total is shown. *Bbs4*<sup>FL/FL</sup> ( $n = 6$  mice), *Vav-iCre Bbs4*<sup>FL/FL</sup> ( $n = 9$ ). (C) Percentage of CD19<sup>+</sup> B cells in spleens and lymph nodes of *Vav-iCre Bbs4*<sup>FL/FL</sup> ( $n = 12$  mice) and *Bbs4*<sup>FL/FL</sup> ( $n = 9$ ) mice, six independent experiments. (D) Percentage of late mature B cells (CD19<sup>+</sup>, IgM<sup>-</sup>, IgD<sup>+</sup>) in spleens of *Vav-iCre Bbs4*<sup>FL/FL</sup> ( $n = 12$  mice), and *Bbs4*<sup>FL/FL</sup> mice ( $n = 9$ ). Representative experiment out of six in total is shown. Statistical significance was calculated using two-tailed Mann–Whitney test,  $P > 0.05$  for all tests. Median is shown.

E Expression of *Cxcl12* and *Il-7* in the bone marrow from *Bbs4*<sup>+/+</sup> *Bbs18*<sup>+/+</sup> (WT) mice (black circles,  $n = 7$  mice), *Bbs4*<sup>+/KO</sup> (Het, green circle,  $n = 3$ ), *Bbs18*<sup>+/KO</sup> (Het, blue circle,  $n = 3$ ), *Bbs4*<sup>KO/KO</sup> (green square,  $n = 5$ ), and *Bbs18*<sup>KO/KO</sup> (blue square,  $n = 2$ ) was analyzed by RT–qPCR in five independent experiments. The expression was normalized to *Gapdh*. The statistical significance of the difference between the BBSome-deficient mice (*Bbs4*<sup>KO/KO</sup> and *Bbs18*<sup>KO/KO</sup>) and controls were calculated using two-tailed Mann–Whitney test. Median is shown.

F MEF cell lines were derived from a single *Bbs4*<sup>+/+</sup> (WT) or a single *Bbs4*<sup>KO/KO</sup> embryos. The expression of *Cxcl12* in these cell lines was analyzed by RT–qPCR. The expression was normalized to *Gapdh* and to *Bbs4*<sup>+/+</sup> MEFs ( $n = 1$ ) for each experiment. Three biological replicates. One sample t-test was used for the statistical analysis.

G Expression of *Cxcl12* and canonical WNT responsive gene *Alpl* in untreated (NT) ST2 cells, or ST2 cells treated with WNT3A or WNT5A was analyzed by RT–qPCR. The expression was normalized to *Gapdh* and untreated ST2 sample ( $n = 1$ ) for each experiment. Four biological replicates were performed. One sample t-test was used for the statistical analysis.

Source data are available online for this figure.

Tanaka et al, 2001; Bullo et al, 2003; Khaodhiar et al, 2004) and adipose tissue (Sindhu et al, 2015). Obesity is also considered as a risk factor for autoimmune disorders (Versini et al, 2014). Indeed, we have shown elevated prevalence of autoimmune disorders (namely T1DM, inflammatory bowel diseases, rheumatoid arthritis, and hypothyroidism) in two independent BBS cohorts. Obesity

potentially contributes to the increased prevalence of autoimmune diseases in BBS patients, as obesity is associated with high prevalence of hypothyroidism, Hashimoto's thyroiditis, and rheumatoid arthritis (Song et al, 2019; Ohno et al, 2020). We also observed alteration of the white blood cell count in BBS patients and in a BBS mouse model. The comparison of BBS patients and non-BBS obese

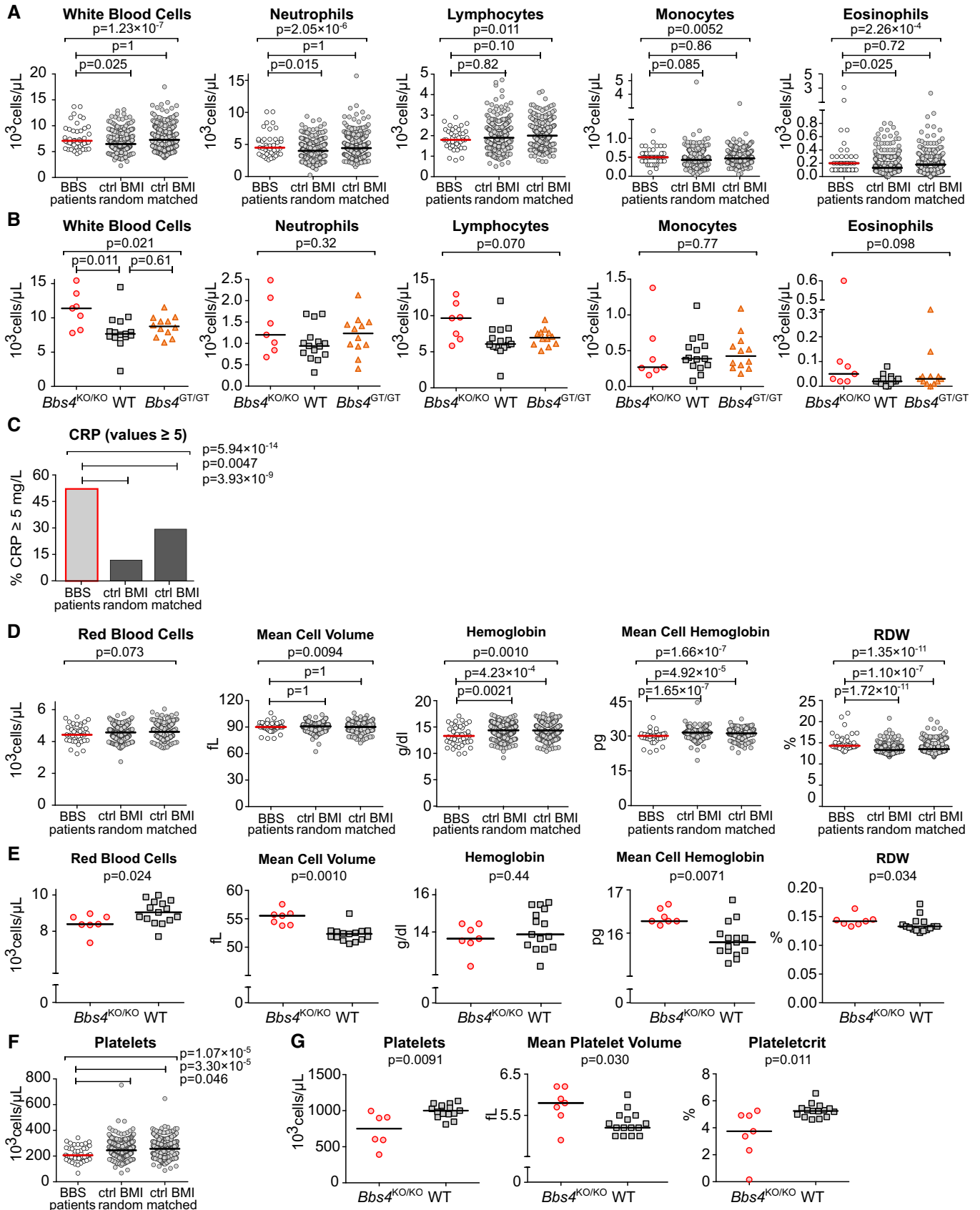


Figure 5.

**Figure 5. Blood homeostasis is altered in BBS patients and *Bbs4*-deficient mice.**

A–G (A, C, D, F) Results of the blood tests of BBS patients from the Guy's Hospital and Great Ormond Street Hospital were extracted from the medical records and compared to two sets of healthy controls obtained from the UK Biobank. The BMI-random controls were age- and gender-matched to the set of BBS patients, with random BMIs. The BMI-matched controls were matched for age, gender, and BMI. BBS patients  $n = 43$  for parameters White blood cell count, Mean cell volume, Hemoglobin and Platelets;  $n = 41$  for parameters Neutrophils, Lymphocytes, Monocytes, Eosinophils;  $n = 39$  for parameters Red blood cells, Mean cell hemoglobin and Red cell distribution width (RDW). Both datasets of healthy controls were selected as 10-fold larger than the set of BBS patients. Median is shown. Kruskal–Wallis test was used for the statistical analysis in (A, D and F). In (C), the percentage of patients or controls having CRP  $\geq 5$  were compared using Fisher's exact test with *post hoc* Sidak correction for multiple comparisons, BBS patients  $n = 42$ . (B, E, G) Indicated parameters were measured using the blood from 20–21 weeks old *Bbs4*<sup>+/+</sup> (WT) ( $n = 15$ ), *Bbs4*<sup>KO/KO</sup> ( $n = 7$ ), and *Bbs4*<sup>GT/GT</sup> ( $n = 12$ ) mice. Kruskal–Wallis test with Dunn's multiple comparison post-tests was used for the statistical analysis. Median is shown.

Source data are available online for this figure.

controls, as well as the comparison of obese and non-obese BBS mouse model, shows that this effect is caused by obesity.

One of the major players in obesity-associated inflammation is leptin, an adipocyte-derived hormone which acts as a pro-inflammatory cytokine (Lord, 2006; Paz *et al*, 2012). The BBSome is proposed to transport the leptin receptor to the plasma membrane, which makes the BBSome-deficient cells unresponsive to leptin (Guo *et al*, 2016). It has been shown that leptin signaling in the central nervous system regulates immune responses and prevents lethal overreaction of the immune system to sepsis in mice (Tschop *et al*, 2010). Thus, it is possible that defective leptin signaling in the nervous system directly contributes to high prevalence of autoimmunity in BBS patients.

Leptin also promotes T-cell activation and proliferation (Martin-Romero *et al*, 2000; Milner & Beck, 2012), suggesting a T-cell intrinsic phenotype of the BBSome deficiency. Moreover, T cells repurpose a number of ciliary transport proteins for immunological synapse formation (Finetti *et al*, 2009; Vivar *et al*, 2016; Stephen *et al*, 2018). Last but not least, the BBSome is functionally connected to IFT20 and SHH signaling components (Wei *et al*, 2012; Williams *et al*, 2014; Nakayama & Katoh, 2018; Niederlova *et al*, 2019), which were shown to regulate early T-cell development (El Abdaloussi *et al*, 2006; Michel *et al*, 2013; Yuan *et al*, 2014; Vivar *et al*, 2016). For all these reasons, we tested whether the BBSome plays a positive or negative intrinsic role in T-cell biology. However, the development and function of T cells were largely unaffected in *Bbs4*<sup>KO/KO</sup> mice and in *Cd4-Cre Bbs4*<sup>FL/FL</sup> mice.

Bardet–Biedl Syndrome patients exhibited additional defects in blood cell homeostasis, which cannot be solely attributed to obesity. First, BBS patients had elevated blood CRP levels, which might be a sign of ongoing inflammation. Second, BBS patients and *Bbs4*-null mice exhibit low platelet counts. Furthermore, platelets from *Bbs4*<sup>KO/KO</sup> mice had larger volume than WT controls. This indicates that a greater fraction of platelets in *Bbs4*<sup>KO/KO</sup> mice are immature. As these mice also have low platelet counts, their bone marrow is likely compensating for platelet loss on the periphery (Stasi, 2012). This state can be a result of immune-mediated processes such as immune thrombocytopenia (Schmoeller *et al*, 2017; Norrasethada *et al*, 2019). Unfortunately, data concerning mean platelet volume are not available for BBS patients, but we can presume that the peripheral destruction of platelets is a cause of thrombocytopenia in BBS patients as well as in mice.

Our analysis of BBS mouse models revealed the role of the BBSome in B-cell development. *Bbs4*<sup>KO/KO</sup>, *Bbs18*<sup>KO/KO</sup>, and non-obese hypomorphic *Bbs4*<sup>GT/GT</sup> mice showed an increased frequency of B-cell precursors in the bone marrow, as well as low numbers of

MZ B cells. These effects were not caused by BBSome deficiency in hematopoietic cells. Instead, BBSome-deficient bone marrow stromal cells produce low levels of CXCL12, most likely as a consequence of enhanced canonical WNT signaling (Gerdes *et al*, 2007; Tamura *et al*, 2011). Our explanation that the BBSome regulates B-cell development by increasing CXCL12 availability is supported by a previous study (Nie *et al*, 2004). This study showed that B-cell-specific deletion of CXCR4, the receptor for CXCL12, manifests with a phenotype resembling our BBS mouse models, i.e., increased frequency in immature IgM<sup>+</sup> IgD<sup>+</sup> B cells in the bone marrow and low numbers of MZ B cells in the spleen. Accordingly, deletion of WBP1L, a negative regulator of CXCR4 signaling, shows the opposite phenotype, i.e., decreased frequency of pre-B cells in the bone marrow and increased frequency of MZ B cells in the spleen (Borna *et al*, 2020). The importance of ciliary signaling in non-hematopoietic bone marrow cells for hematopoiesis should be addressed in further studies.

To our knowledge, this is the first study revealing the dysregulation of the immune and hematopoietic systems in patients suffering from a ciliopathy. Obesity, a common feature of ciliopathies such as BBS and Alström syndrome (Vaisse *et al*, 2017), leads to elevated concentration of white blood cells in BBS patients. However, BBS patients also exhibit elevated blood CRP levels and low platelet counts in an obesity-independent manner. A detailed analysis of BBS mouse models revealed low CXCL12 production by BBSome-deficient stromal cells resulting in defects in B-cell development. Given the importance of the CXCL12–CXCR4 axis in immunity and hematopoiesis, there might be additional effects of BBSome deficiency beyond our findings. Altogether, we identified BBS as a risk factor for autoimmune diseases.

## Materials and Methods

### Antibodies and reagents

Antibodies to the following antigens were used for flow cytometry: CD1d Pe-Cy7 (1B1, #123524, Biolegend), CD4 BV650 (RM4-5, #100545, Biolegend), CD8a PE-Cy7 (53-6.7, #1103610, SONY), CD8a FITC (53-6.7, #100706, Biolegend), CD19 PE (6D5, #115508, Biolegend), CD23 APC (b3b4, #1108095, SONY), CD24 FITC (M1/69, #101806, Biolegend), CD43 PE (S7, #553271, BD PharMingen), CD44 PE (IM7, #103008, Biolegend), B220 Alexa Fluor 700 (RA3-6B2, #103231, Biolegend), B220 FITC (RA3-6B2, #103206, Biolegend), CD69 PE (H1.2F3, #104508, Biolegend), CD69 FITC (H1.2F3, #104506, Biolegend), IgM BV421 (rmm-1, #2632585,

SONY), IgD Per-CP-Cy5.5 (11-26c.2a, #2628545, SONY), IgL $\lambda$  APC (RML-42, #407306, Biologend), TCR $\beta$  APC (H57-597, #109212, Biologend).

Antibodies used for immunoblot analysis: BBS4 (rabbit, a kind gift from Prof. Maxence Nachury, UCSF, CA, USA, recognizing LQVGEALVWTKPKVKDPKSKH peptide in exon 15 of human BBS4),  $\beta$ -actin (mouse, #4967, Cell Signaling), anti-FLAG (M2, mouse, F1804-200UG, SIGMA),  $\alpha$ -mouse HRP,  $\alpha$ -rabbit HRP (both from Jackson ImmunoResearch).

Antibodies used for lymphocyte enrichment: biotinylated  $\alpha$ -TCR $\beta$  (H57-597, #553169, BD PharMingen),  $\alpha$ -CD19 (6D5, #115503, Biologend).

Antibody used for B-cell activation: polyclonal F(ab')<sub>2</sub>-Goat anti-Mouse IgM (Mu chain), a kind gift from Dr. Tomas Brdicka (Institute of Molecular Genetics of the Czech Academy of Sciences in Prague, henceforth IMG).

Dyes and reagents: 4-hydroxy-3-nitrophenylacetic acid succinimide ester (LGC, Biosearch Technologies), peptides OVA (SIINFELK), Q4R7 (SIIRFERL), Q4H7 (SIIRFEHL), T4 (SIITFEKL) (Eurogentec or Peptides&Elephants), CFSE and DDAO cell tracker dyes (both Invitrogen), LIVE/DEAD near-IR dye (Life Technologies), Hoechst 33258 (Life Technologies).

## Mice

All mice were 5–25 weeks old and had C57Bl/6J background if not indicated otherwise. Mice were bred in specific-pathogen-free facility (IMG) (Flachs *et al*, 2014). Animal protocols were approved by the Czech Academy of Sciences, in accordance with the laws of the Czech Republic. Males and females were used for the experiments. If possible, age- and sex-matched pairs of animals were used in the experimental groups. If possible, littermates were equally divided into the experimental groups. No randomization was performed since the experimental groups were based solely on the genotype of the mice. In case of the RIP.OVA mice used for the autoimmune diabetes model, mice were assigned to experimental groups randomly (defined by their ID numbers) prior to the visual contact between the experimenter and the mice. The experiments were not blinded since no subjective scoring method was used. For animal studies, minimal sample size was estimated using resource equation approach. As the number of mutant mice was limited due to pre-weaning lethality, all the available mutant mice (and their WT littermates) were used for experiments. For the diabetes experiments, the number of mice was estimated based on our previous experience with this method.

B1–8 (Sonoda *et al*, 1997), RIP.OVA (Kurts *et al*, 1998), OT-I *Rag2*<sup>KO/KO</sup> (Palmer *et al*, 2016), *Vav-iCre* (Shimshak *et al*, 2002; de Boer *et al*, 2003), *Cd4-Cre* (Lee *et al*, 2001) strains were described previously. Mouse *Bbs4*<sup>tm1a(EUCOMM)Hmgu</sup> allele with a gene trap cassette (abbreviated as *Bbs4*<sup>GT</sup>) was obtained from KOMP (UC Davis, CA, USA) as frozen sperm and used for *in vitro* fertilization. *Bbs4*<sup>tm1a(EUCOMM)Hmgu</sup> mice were crossed with a Flp-deleter mouse strain, *Gt(ROSA)26Sor*<sup>tm2(CAG-Flpo,-EYFP)lcs</sup> (MGI: 5285396, Philippe Soriano), in order to obtain exon 6 flanked by LoxP sites for conditional or germ line *Bbs4* ablation (*Bbs4*<sup>tm1c(EUCOMM)Hmgu</sup>). In order to generate germ line knock-out mice, the exon 6 was removed by a general Cre-deleter strain, *Gt(ROSA)26Sor*<sup>tm1(ACTB-cre,-EGFP)lcs</sup> (MGI: 5285392, Philippe Soriano), resulting in *Bbs4*<sup>tm1d(EUCOMM)Hmgu</sup>

(abbreviated as *Bbs4*<sup>KO</sup>) as described previously (Skarnes *et al*, 2011). *Bbs4*<sup>+/+</sup> and *Bbs4*<sup>GT/GT</sup> or *Bbs4*<sup>KO/KO</sup> littermates were generated by intercrossing heterozygous animals.

Mice with a null-mutation in *Bbs18* (alias *Bbip1*) were generated in a C57BL/6N background using a CRISPR genome-editing system. For this purpose, Cas9 protein and gene-specific single guide (sg) RNAs (Integrated DNA Technologies, Coralville, IA, USA) were used for a zygote electroporation using a protocol described previously (Chen *et al*, 2016). sgRNA sequences with the PAM motif in bold (3' end) were as follows:

sgRNA target 1: CTCTTCCTGAAAATCGGTG**AGG**

sgRNA target 2: GGAATAACCAACTGGTCTT**AGG**

The correct genome editing was confirmed by PCR amplification in the founder mouse with the primers listed in Appendix Table S5. Generation of *Bbs18* KO mice was part of the International Mouse Phenotyping Consortium project (mouse ID 12685, *Bbip1*<sup>em1(IMPC)Cpcz</sup>). The mutant allele was backcrossed for two generations to C57BL/6N mice and for one generation to C57BL/6J mice.

We did not confirm the efficacy of the *Bbs4* deletion in *Bbs4*<sup>FL/FL</sup> *Vav-iCre* strain. However, this *Vav-iCre* mouse line was proven as an efficient gene deleter in the hematopoietic bone marrow cells and splenocytes in our facility previously (Kardosova *et al*, 2018).

## Cell culture

T2-Kb is a H-2Kb transgenic subline of the TAP1 $\gamma$ 2-deficient line (Alexander *et al*, 1989). The bone marrow-derived stroma cell line, ST2, was kindly provided by Dr. Jana Balounova (IMG). The HEK293T cells were kindly provided by Dr. Tomas Brdicka (IMG). All cell lines were tested for Mycoplasma contamination by PCR on a regular basis. MEF cells were derived from E13.5 mouse embryos. After the removal of the placenta, yolk sac, head, liver, and heart, the tissue was trypsinized and homogenized. The adherent MEFs were genotyped and cultured. All cell lines were cultivated in DMEM supplemented with 10% fetal calf serum (FCS; Gibco), 100 U/ml penicillin (BB Pharma), 100  $\mu$ g/ml streptomycin (Sigma-Aldrich), and 40  $\mu$ g/ml gentamicin (Sandoz).

## Cloning, transfection, and generation of BBS4-deficient cell lines

*Bbs4* WT and GT ORFs were amplified from cDNA obtained from the kidney of respective mice. FLAG-tag was fused to the *Bbs4* WT and GT C-terminally and cloned into pXJ41 vector (kindly provided by Dr. Tomas Brdicka, IMG) using EcoRI/XhoI restriction sites.

HEK293T cells at ~50% confluency were transfected with the *Bbs4* WT or *Bbs4* GT encoding pXJ41 plasmid using the following protocol. Thirty microgram of DNA plasmid was mixed with 75  $\mu$ g polyethylenimine in 0.5 ml of 0.5% serum antibiotic-free media for 10 min at room temperature. The mixture was then added onto cells in 3 ml of 0.5% serum and antibiotic-free media. The media was replaced by DMEM with 10% serum and antibiotics after 3 h. Twenty-four hours after transfection, the expression of BBS4 was analyzed by  $\alpha$ -FLAG antibody via immunoblotting.

BBS4-deficient ST2 cell lines were generated using the CRISPR/Cas9 approach. sgRNA targeting mouse *Bbs4* gene (NM\_175325.3) was designed using the CHOPCHOP tool (Labun *et al*, 2019). sgRNA was cloned into pSpCas9(BB)-2A-GFP (PX458) vector kindly

provided by Dr. Feng Zhang (Addgene plasmid #48138) (Ran *et al*, 2013). sgRNA sequences with the PAM motif in bold (3' end) for mouse *BBS4* are as follows:

Mouse *BBS4* sgRNA#1: CATAATCCTTCCGGATATAGTGG

Mouse *BBS4* sgRNA#2: GCACTGATTTTCGCTGGAAGG

ST2 cells were transfected with PX458 vector with the *BBS4* sgRNA using Lipofectamine (Invitrogen). After 48 h, GFP positive cells were sorted as single cells in 96-well plates using the 488nm laser on FACS Aria IIu (BD Bioscience). Clones were analyzed for the expression of *BBS4* proteins by immunoblotting and sequencing of DNA surrounding the sgRNA target site.

### In vitro stimulation with WNT

Confluent ST2 cells were stimulated with 5 ng/ml recombinant mouse WNT-3A (RD System) or 200 ng/ml WNT-5A (Sigma), or left unstimulated in DMEM supplemented with 10% FCS (Gibco), 100 U/ml penicillin (BB Pharma), 100 µg/ml streptomycin (Sigma-Aldrich), and 40 µg/ml gentamicin (Sandoz) for 48 h at 37°C/CO<sub>2</sub> incubator. Total RNA was extracted from the cells, and *Il-7*, *Cxcl12*, and *Alpl* mRNA expression level was determined by qRT-PCR.

### RT-qPCR and end-point PCR

Total RNA was extracted from tissues (kidney, brain, lymph nodes, spleen, bone marrow) and T cells from indicated mice, ST2 cells or mouse embryonic fibroblasts using Trizol LS (Invitrogen, # 10296010) and transcribed using RevertAid reverse transcriptase (Thermo Fisher, # EP0442) with oligo(dT)<sub>18</sub> primers according to the manufacturer's instructions. cDNA was used for end-point PCR or quantitative PCR using indicated primers (primer sequences are listed in the Appendix Table S5). Samples for quantitative PCR were measured by LightCycler 480 (Roche) in technical triplicates. Obtained C<sub>T</sub> values were normalized to indicated reference genes.

### Enrichment of T and B lymphocytes

T and B lymphocytes for immunoblotting were enriched by positive selection using the Dynabeads Biotin Binder kit (Invitrogen, #11047), and biotinylated α-TCRβ and α-CD19 antibodies, respectively. B cells for B-cell activation assay were enriched by negative selection using biotinylated α-CD4 and α-CD8 antibodies with the automated cell separator AutoMACS Pro system (Miltenyi Biotec).

### Immunoblotting

For analysis of *BBS4* expression, freshly isolated murine organs (testicles, thymi, brain), enriched lymphocytes, ST2 cells, or HEK293T cells were lysed and denatured in Laemmli buffer supplemented with 20mM dithiothreitol. The resulting lysates were separated on a polyacrylamide gel and transferred to nitrocellulose membrane using standard immunoblotting protocols. Membranes were probed with indicated antibodies followed by secondary anti-rabbit or anti-mouse HRP-conjugated antibodies. Staining for β-actin served as a loading control. The signal was visualized using

chemiluminescence immunoblot imaging system Azure c300 (Azure Biosystems, Inc.).

### Histological analysis

Testes isolated from 30-day-old male mice were collected, immediately dipped into Bouin solution, and fixed for 24 h at 4°C. Paraffin-embedded tissue blocks were cut with a microtome (Leica RM2255), and the sections were stained with hematoxylin/eosin using standard technique. The images were taken using microscope system Axioplan 2 imaging (Zeiss) using 10×/0.50 NA objective.

### Weighting of mice

Bodyweight of *Bbs4*<sup>+/+</sup>, *Bbs4*<sup>GT/GT</sup>, *Bbs4*<sup>KO/KO</sup> mice was recorded weekly starting at 5 weeks of age. All the mice were kept in sex-matched cages together with their littermates (≤ 6 per cage) and fed a standard chow diet ad libitum.

### ELISA

Blood from *Bbs4*<sup>KO/KO</sup>, *Bbs4*<sup>GT/GT</sup>, and their age/sex-matched controls was collected by submandibular bleeding (Golde *et al*, 2005) into EDTA-coated tubes and centrifuged for 15 min at 1,000 g at 4°C in order to separate plasma. Obtained plasma samples were assayed immediately or stored at -80°C for later use. Leptin concentration was measured by mouse leptin ELISA Kit (Cloud-Clone Corp., SEA084Mu) according to the manufacturer's instructions.

### Flow cytometry

Live cells were stained with the above-listed antibodies on ice. LIVE/DEAD near-IR dye or Hoechst 33258 were used for discrimination of live and dead cells. Flow cytometry was carried out using an LSRII (BD Bioscience). Data were analyzed using FlowJo software (TreeStar).

### B-cell activation

For activation of nitrophenyl-specific B cells, splenocytes isolated from B1-8 mice (*Bbs4*<sup>+/+</sup> and *Bbs4*<sup>GT/GT</sup>) were mixed with 4-hydroxy-3-nitrophenylacetic acid succinimide ester (NP-Osu)-loaded T2-Kb cells at 1:10 or 1:3 ratios, and incubated in DMEM supplemented with 10% FCS (Gibco), 100 U/ml penicillin (BB Pharma), 100 µg/ml streptomycin (Sigma-Aldrich), and 40 µg/ml gentamicin (Sandoz) for 6 h at 37°C/CO<sub>2</sub> incubator.

For activation of *Bbs4*<sup>KO/KO</sup> B cells, spleens and lymph nodes were isolated from *Bbs4*<sup>KO/KO</sup> and control (*Bbs4*<sup>+/KO</sup> or *Bbs4*<sup>+/+</sup>) mice, and B cells were enriched by negative selection using automated cell separator AutoMACS. B cells were stimulated by indicated dose of plastic-bounded F(ab')<sub>2</sub>-Goat anti-Mouse IgM (Mu chain) antibody in 96 well plate in DMEM supplemented with 10% FCS (Gibco), 100 U/ml penicillin (BB Pharma), 100 µg/ml streptomycin (Sigma-Aldrich), and 40 µg/ml gentamicin (Sandoz) overnight at 37°C/CO<sub>2</sub> incubator.

After incubation, cells were centrifuged (1,000 g, 2 min), resuspended in PBS/0.5% gelatin, stained with antibodies (CD19, B220, IgLλ, CD69) for 30 min on ice, and analyzed by flow cytometry.

### T-cell conjugation assay

T-cell conjugation assay was performed as previously shown (Palmer *et al*, 2016). Briefly, OT-I T cells from *Bbs4<sup>FL/FL</sup> Cd4-Cre<sup>-</sup>* or *Bbs4<sup>FL/FL</sup> Cd4-Cre<sup>+</sup>* littermates were stained with CFSE cell tracker dye, and splenocytes isolated from C57Bl/6 mice were stained with DDAO cell tracker dye. Splenocytes were loaded with OVA peptide or with indicated altered peptide ligands for 3 h in RPMI/10% FCS, mixed with OT-I T cells at 2:1 ratio, and centrifuged (1,000 g, 1 min). After 20 min of co-culture at 37°C/CO<sub>2</sub> incubator, cells were fixed by adding formaldehyde (2% final, 35 min). Cells were centrifuged (1,000 g, 2 min), resuspended in PBS/0.5% gelatin, and analyzed by flow cytometry. The result of each of the four biological replicates was an average of technical duplicates.

### Model of autoimmune diabetes

The model of autoimmune diabetes has been described previously (Drobek *et al*, 2018). Briefly, OT-I cells from *Bbs4<sup>FL/FL</sup> Cd4-Cre<sup>-</sup>* or *Bbs4<sup>FL/FL</sup> Cd4-Cre<sup>+</sup>* sex-matched littermates were adoptively transferred into a host RIP.OVA mice intravenously. On the following day, the host mice were immunized with 5,000 CFU of OVA expressing *Listeria monocytogenes* (Lm). Lm strain expressing OVA has been described previously (Chan *et al*, 2013). Level of glucose in the urine of RIP.OVA mice was monitored on a daily basis using test strips (GLUKOPHAN, Erba Lachema).

The animal was considered to suffer from diabetes when the concentration of glucose in the urine reached  $\geq 1,000$  mg/dl for two consecutive days. On day 7 post-infection, blood glucose was measured using contour blood glucose meter (Bayer).

### Blood analysis

Blood from 20–21 weeks old *Bbs4<sup>+/+</sup>*, *Bbs4<sup>KO/KO</sup>*, and *Bbs4<sup>GT/GT</sup>* mice was collected by submandibular bleeding (Golde *et al*, 2005) into EDTA-coated tubes and analyzed using BC5300 Vet Auto Hematology Analyzer (Mindray Bio-Medical Electronics Co., Ltd.).

### Analysis of the clinical data of BBS patients

Fully anonymized medical records of 255 BBS patients were obtained from the Clinical Registry Investigating BBS (CRIBBS) by the NIH through the National Center for Advancing Translational Sciences and the Office of Rare Diseases Research (<https://grdr.hms.harvard.edu/transmart>). Data were extracted from the following categories of the CRIBBS: Clinical data/ Physical findings/ Bone and joint information, Endocrine, Thyroid disorders, Digestive. Although the CRIBBS registry does not contain information about the specific type of arthritis, we assume that the arthritis reported in can be classified as rheumatoid arthritis due to the following facts: (i) the mean age of onset of arthritis in the CRIBBS cohort is 28.7 years, (ii) the mean age on onset of rheumatoid arthritis in general population is 20–29 years (Hayter & Cook, 2012), (iii) the typical onset of osteoarthritis is after 50 years (Martel-Pelletier *et al*, 2016).

Medical records of BBS patients attending the BBS multidisciplinary clinic at Guy's Hospital of Guy's and St Thomas' NHS Foundation Trust, London, or Great Ormond Street Hospital, London,

were studied in detail with focus on presence of any immune-related phenotype. In addition to the manual control, the records were also automatically searched for the occurrence of the following terms: autoimm-, immun-, thyro-, inflam-, diabet-, T1DM, ulcerative, crohn, IBD, rheuma-, arthri-, joints.

Data about the prevalence of autoimmune diseases in the two BBS cohorts were compared to normal prevalence of autoimmune diseases reported in the Autoimmune Registry or relevant publications in case of location-specific prevalence of hypothyroidism and inflammatory bowel diseases (Stone *et al*, 2003; Hayter & Cook, 2012; Taylor *et al*, 2018). Statistical significance of the difference in the prevalence between the BBS patients and overall population was tested using two-tailed exact binomial test in RStudio (function `binom.test`, R version: 3.6.2, RStudio version: 1.2.1335). The respective R-script is deposited in Zenodo (<https://doi.org/10.5281/zenodo.3733230>).

Results of blood tests of BBS patients (total white blood cell count, leukocyte populations, hemoglobin, platelet counts, mean corpuscular volume, red blood cell count, hematocrit, red cell distribution width and mean corpuscular hemoglobin), their age ranges, genes with causative mutation and body mass indices (BMI) were retrospectively ascertained from medical records stored at the BBS multidisciplinary clinic at Guy's Hospital of Guy's and St Thomas' NHS Foundation Trust, London, or Great Ormond Street Hospital, London. Blood tests were performed during regular medical examination of the patients.

Two distinct sets of controls for the analyzed set of BBS patients were selected from the 14,750 participants of the UK Biobank project (ID: 40103) (Sudlow *et al*, 2015). First, we selected 10 controls for each patient matching by age range (categories 41–50, 51–60, 60+ years) and sex. These controls had random BMI and thus were used as BMI-random controls. Second, we selected 10 controls for each patient matching by age range (categories 41–50, 51–60, 60+ years), sex, and BMI. These were used as BMI-matched controls. For 34 of the 42 patients, we found controls with BMI difference  $\leq 0.6$  kg/m<sup>2</sup>. For the eight patients with extreme BMI values, that precise matching was not possible, so that we selected the best-matching controls available for these cases. As the UK Biobank only includes participants older than 40 years, only BBS patients from this age group were included to this analysis.

All BBS patients gave informed consent or assent. The protocol for this study was approved by the Great Ormond Street Hospital Research Ethics Committee (Project Molecular Genetics of Human Birth Defects—mapping and gene identification, reference #08/H0713/82) and by the ethical committee of the IMG.

### Statistical analyses

The statistical significance of the observed differences between experimental groups was calculated using frequentist statistics. Appropriate tests were applied for particular experiments, and *P*-values were calculated using R or Prism 5.04 (GraphPad). The names of the tests are indicated in the Figure Legends. The *P*-values are indicated in the Figures or in the Figure Legends. Two-sided tests were used. We adjusted *P*-values for multiple comparisons, when applicable. Whenever possible, we used non-parametric tests. The only exceptions were RT-qPCR experiments

with very low number of replicates, where non-parametric tests were not applicable. In these cases we used one sample *t*-test, assuming normal distribution of the data (which could not be statistically tested because of low number of replicates). We indicate the exact *P*-value with the exception of some tests where the statistical software did not calculate the exact *P*-value if it was very small ( $P < 0.0001$ ).

## Data availability

No primary large datasets have been generated or deposited. R-scripts used for the analysis of human patient data were deposited in Zenodo (<https://doi.org/10.5281/zenodo.3733230>).

**Expanded View** for this article is available online.

## Acknowledgements

We thank Ladislav Cupak for technical assistance and genotyping of mice and Dr. Alena Moudra for the assistance with *Listeria* infection. We are thankful to all colleagues who provided us reagents and cell lines. This study was supported by the Czech Science Foundation (17-20613Y to MH), and the Charles University Grant Agency (1706119 to OT), and the National Institute for Health Research Biomedical Research Centre at Great Ormond Street Hospital for Children NHS Foundation Trust and University College London. The Group of Adaptive Immunity is supported by an EMBO Installation Grant (3259 to OS) and the Institute of Molecular Genetics of the Czech Academy of Sciences core funding (RVO 68378050). This research has been conducted using the UK Biobank Resource under application number #40103. OS is supported by the Purkyne Fellowship provided by the Czech Academy of Sciences. OT, VN, and AP are students partially supported by the Faculty of Science, Charles University, Prague. The graphical abstract was created with BioRender.com. The *BBS18*<sup>-/-</sup> mouse model was prepared in the Czech Centre for Phenogenomics supported by following grants: LM2015040, LM2018126, OP RDI CZ.1.05/2.1.00/19.0395, OP RDI BIOCEV CZ.1.05/1.1.00/02.0109 provided by the Czech Ministry of Education, Youth and Sports and the European Regional Development Fund. Grantová Agentura České Republiky (GAČR) (17-20613Y), Grantová Agentura, Univerzita Karlova (GA UK) (1706119), European Molecular Biology Organization (3259), Akademie Věd České Republiky (CAS) (RVO 68378050), Czech Academy of Sciences, Purkyne Fellowship, Charles University, Faculty of Science, Ministerstvo Školství, Mládeže a Tělovýchovy (MŠMT) (LM2015040, LM2018126, OP RDI CZ.1.05/2.1.00/19.0395, OP RDI BIOCEV CZ.1.05/1.1.00/02.0109)

## Author contributions

MH and OS conceived the study and were in charge of the overall direction and planning. OT, VN, AD, AP, and OS performed the animal experiments. OT, AP, and MH performed experiments with cell lines. EF, KS, and PB collected the data of BBS patients from the Great Ormond Street Hospital and Guy's Hospital in London. VN filtered and analyzed the patients' data. PK, JP, and RS generated *Bbs18*<sup>KO/KO</sup> mouse. ZT contributed to the histological analysis of murine testes. OT, VN, and OS wrote the first draft of the manuscript. OT, VN, AP, MH, and OS wrote the final version of the manuscript with the contribution of all the other authors.

## Conflict of interest

The authors declare that they have no conflict of interest.

## References

- Alexander J, Payne JA, Murray R, Frelinger JA, Cresswell P (1989) Differential transport requirements of Hla and H-2 class-I glycoproteins. *Immunogenetics* 29: 380–388
- Beales PL, Elcioglu N, Woolf AS, Parker D, Flinter FA (1999) New criteria for improved diagnosis of Bardet-Biedl syndrome: results of a population survey. *J Med Genet* 36: 437–446
- Berbari NF, Lewis JS, Bishop GA, Askwith CC, Mykytyn K (2008) Bardet-Biedl syndrome proteins are required for the localization of G protein-coupled receptors to primary cilia. *Proc Natl Acad Sci USA* 105: 4242–4246
- de Boer J, Williams A, Skavdis G, Harker N, Coles M, Tolaini M, Norton T, Williams K, Roderick K, Potocnik AJ et al (2003) Transgenic mice with hematopoietic and lymphoid specific expression of Cre. *Eur J Immunol* 33: 314–325
- Borna S, Drobek A, Kralova J, Glatzova D, Splichalova I, Fabisik M, Pokorna J, Skopcova T, Angelisova P, Kanderova V et al (2020) Transmembrane adaptor protein WBP1L regulates CXCR4 signalling and murine haematopoiesis. *J Cell Mol Med* 24: 1980–1992
- Bullo M, Garcia-Lorda P, Megias I, Salas-Salvado J (2003) Systemic inflammation, adipose tissue tumor necrosis factor, and leptin expression. *Obes Res* 11: 525–531
- Chan SSM, Luben R, Olsen A, Tjonneland A, Kaaks R, Teucher B, Lindgren S, Grip O, Key T, Crowe FL et al (2013) Body mass index and the risk for Crohn's disease and ulcerative colitis: data from a European prospective cohort study (The IBD in EPIC Study). *Am J Gastroenterol* 108: 575–582
- Chen S, Lee B, Lee AYF, Modzelewski AJ, He L (2016) Highly efficient mouse genome editing by CRISPR ribonucleoprotein electroporation of zygotes. *J Biol Chem* 291: 14457–14467
- Crompton T, Outram SV, Hager-Theodorides AL (2007) Sonic hedgehog signalling in T-cell development and activation. *Nat Rev Immunol* 7: 726–735
- Davis RE, Swiderski RE, Rahmouni K, Nishimura DY, Mullins RF, Agassandian K, Philp AR, Searby CC, Andrews MP, Thompson S et al (2007) A knockin mouse model of the Bardet-Biedl syndrome 1 M390R mutation has cilia defects, ventriculomegaly, retinopathy, and obesity. *Proc Natl Acad Sci USA* 104: 19422–19427
- De Rosa V, Procaccini C, Cali G, Pirozzi G, Fontana S, Zappacosta S, La Cava A, Matarese G (2007) A key role of leptin in the control of regulatory T cell proliferation. *Immunity* 26: 241–255
- Drakopoulou E, Outram SV, Rowbotham NJ, Ross SE, Furmanski AL, Saldana JJ, Hager-Theodorides AL, Crompton T (2010) Non-redundant role for the transcription factor Gli1 at multiple stages of thymocyte development. *Cell Cycle* 9: 4144–4152
- Drobek A, Moudra A, Mueller D, Huranova M, Horkova V, Pribikova M, Ivanek R, Oberle S, Zehn D, McCoy KD et al (2018) Strong homeostatic TCR signals induce formation of self-tolerant virtual memory CD8 T cells. *Embo J* 37
- El Abdaloussi E, Graves S, Meng FY, Mandal M, Mashayekhi M, Aifantis I (2006) Hedgehog signaling controls thymocyte progenitor homeostasis and differentiation in the thymus. *Nat Immunol* 7: 418–426
- Finetti F, Paccani SR, Riparbelli MG, Giacomello E, Perinetti G, Pazour GJ, Rosenbaum JL, Baldari CT (2009) Intraflagellar transport is required for polarized recycling of the TCR/CD3 complex to the immune synapse. *Nat Cell Biol* 11: 1332–1339
- Finetti F, Paccani SR, Rosenbaum J, Baldari CT (2011) Intraflagellar transport: a new player at the immune synapse. *Trends Immunol* 32: 139–145

- Finetti F, Patrussi L, Masi G, Onnis A, Galgano D, Lucherini OM, Pazour GJ, Baldari CT (2014) Specific recycling receptors are targeted to the immune synapse by the intraflagellar transport system. *J Cell Sci* 127: 1924–1937
- Flachs P, Bhattacharyya T, Mihola O, Pialek J, Forejt J, Trachtulec Z (2014) Prdm9 Incompatibility controls oligospermia and delayed fertility but no selfish transmission in mouse intersubspecific hybrids. *PLoS One* 9: e95806
- Forsythe E, Kenny J, Bacchelli C, Beales PL (2018) Managing Bardet-Biedl syndrome—now and in the future. *Front Pediatr* 6: 23
- Furmanski AL, Saldana JL, Ono M, Sahni H, Paschalidis N, D'Acquisto F, Crompton T (2013) Tissue-derived hedgehog proteins modulate Th differentiation and disease. *J Immunol* 190: 2641–2649
- Georgiades P, Ogilvy S, Duval H, Licence DR, Charnock-Jones DS, Smith SK, Print CG (2002) VavCre transgenic mice: a tool for mutagenesis in hematopoietic and endothelial lineages. *Genesis* 34: 251–256
- Gerdes JM, Liu Y, Zaghoul NA, Leitch CC, Lawson SS, Kato M, Beachy PA, Beales PL, DeMartino GN, Fisher S et al (2007) Disruption of the basal body compromises proteasomal function and perturbs intracellular Wnt response. *Nat Genet* 39: 1350–1360
- Goetz SC, Bangs F, Barrington CL, Katsanis N, Anderson KV (2017) The Meckel syndrome-associated protein MKS1 functionally interacts with components of the BBSome and IFT complexes to mediate ciliary trafficking and hedgehog signaling. *PLoS One* 12: e0173399
- Golde WT, Gollobin P, Rodriguez LL (2005) A rapid, simple, and humane method for submandibular bleeding of mice using a lancet. *Lab Animal* 34: 39–43
- Granata M, Skarmoutsou E, Trovato C, Rossi GA, Mazzarino MC, D'Amico F (2017) Obesity, Type 1 diabetes, and psoriasis: an autoimmune triple flip. *Pathobiology* 84: 71–79
- Gremese E, Toluoso B, Gigante MR, Ferraccioli G (2014) Obesity as a risk and severity factor in rheumatic diseases (autoimmune chronic inflammatory diseases). *Front Immunol* 5: 576
- Guo DF, Beyer AM, Yang BL, Nishimura DY, Sheffield VC, Rahmouni K (2011) Inactivation of Bardet-Biedl syndrome genes causes kidney defects. *Am J Physiol-Renal* 300: F574–F580
- Guo DF, Cui HX, Zhang QH, Morgan DA, Thedens DR, Nishimura D, Grobe JL, Sheffield VC, Rahmouni K (2016) The BBSome controls energy homeostasis by mediating the transport of the leptin receptor to the plasma membrane. *Plos Genet* 12: e1005890
- Halac U, Herzog D (2012) Bardet-Biedl Syndrome, Crohn Disease, primary sclerosing cholangitis, and autoantibody positive thyroiditis: a case report and a review of a cohort of BBS patients. *Case Rep Med* 2012: 209827
- Hayter SM, Cook MC (2012) Updated assessment of the prevalence, spectrum and case definition of autoimmune disease. *Autoimmun Rev* 11: 754–765
- Jin H, White SR, Shida T, Schulz S, Aguiar M, Gygi SP, Bazan JF, Nachury MV (2010) The conserved Bardet-Biedl Syndrome proteins assemble a coat that traffics membrane proteins to cilia. *Cell* 141: 1208–1219
- Johnson AR, Milner JJ, Makowski L (2012) The inflammation highway: metabolism accelerates inflammatory traffic in obesity. *Immunol Rev* 249: 218–238
- Kardosova M, Zjablovskaja P, Danek P, Angelisova P, de Figueiredo-Pontes LL, Welner RS, Brdicka T, Lee S, Tenen DG, Alberich-Jorda M (2018) C/EBP gamma is dispensable for steady-state and emergency granulopoiesis. *Haematologica* 103: E331–E335
- Kepler-Noreuil KM, Blumhorst S, Sapp JC, Brinckman D, Johnston J, Nopoulos PC, Biesecker LG (2011) Brain tissue- and region-specific abnormalities on volumetric MRI scans in 21 patients with Bardet-Biedl syndrome (BBS). *Bmc Med Genet* 12: 101
- Khaodhiar L, Ling PR, Blackburn GL, Bistran BR (2004) Serum levels of interleukin-6 and C-reactive protein correlate with body mass index across the broad range of obesity. *JPEN J Parenter Enteral Nutr* 28: 410–415
- King CG, Koehli S, Hausmann B, Schmalzer M, Zehn D, Palmer E (2012) T cell affinity regulates asymmetric division, effector cell differentiation, and tissue pathology. *Immunity* 37: 709–720
- Klink BU, Zent E, Juneja P, Kuhlee A, Raunser S, Wittinghofer A (2017) A recombinant BBSome core complex and how it interacts with ciliary cargo. *Elife* 6: e27434
- Kurts C, Miller JFAP, Subramaniam RM, Carbone FR, Heath WR (1998) Major histocompatibility complex class I-restricted cross-presentation is biased towards high dose antigens and those released during cellular destruction. *J Exp Med* 188: 409–414
- La Cava A (2017) Leptin in inflammation and autoimmunity. *Cytokine* 98: 51–58
- Labun K, Montague TG, Krause M, Cleuren YNT, Tjeldnes H, Valen E (2019) CHOPCHOP v3: expanding the CRISPR web toolbox beyond genome editing. *Nucleic Acids Res* 47: W171–W174
- Lee PP, Fitzpatrick DR, Beard C, Jessup HK, Lehar S, Makar KW, Perez-Melgosa M, Sweetser MT, Schlissel MS, Nguyen S et al (2001) A critical role for Dnmt1 and DNA methylation in T cell development, function, and survival. *Immunity* 15: 763–774
- Lindstrand A, Davis EE, Carvalho CM, Pehlivan D, Willer JR, Tsai IC, Ramanathan S, Zuppan C, Sabo A, Muzny D et al (2014) Recurrent CNVs and SNVs at the NPHP1 locus contribute pathogenic alleles to Bardet-Biedl syndrome. *Am J Hum Genet* 94: 745–754
- Lindstrand A, Frangakis S, Carvalho CMB, Richardson EB, McFadden Kelsey A, Willer Jason R, Pehlivan D, Liu P, Padiaditakis Igor L, Sabo A et al (2016) Copy-number variation contributes to the mutational load of Bardet-Biedl Syndrome. *Am J Hum Genet* 99: 318–336
- Liu PW, Lechtreck KF (2018) The Bardet-Biedl syndrome protein complex is an adapter expanding the cargo range of intraflagellar transport trains for ciliary export. *Proc Natl Acad Sci USA* 115: E934–E943
- Lord GM (2006) Leptin as a proinflammatory cytokine. *Contrib Nephrol* 151: 151–164
- Martel-Pelletier J, Barr AJ, Cicuttini FM, Conaghan PG, Cooper C, Goldring MB, Goldring SR, Jones G, Teichtahl AJ, Pelletier JP (2016) Osteoarthritis. *Nat Rev Dis Primers* 2: 16072
- Martin-Romero C, Santos-Alvarez J, Goberna R, Sanchez-Margalet V (2000) Human leptin enhances activation and proliferation of human circulating T lymphocytes. *Cell Immunol* 199: 15–24
- Michel KD, Uhmman A, Dressel R, van den Brandt J, Hahn H, Reichardt HM (2013) The Hedgehog receptor patched1 in T Cells is dispensable for adaptive immunity in mice. *PLoS One* 8: e61034
- Milner JJ, Beck MA (2012) The impact of obesity on the immune response to infection. *Proc Nutr Soc* 71: 298–306
- Moro K, Yamada T, Tanabe M, Takeuchi T, Ikawa T, Kawamoto H, Furusawa J, Ohtani M, Fujii H, Koyasu S (2010) Innate production of T(H)2 cytokines by adipose tissue-associated c-Kit(+)Sca-1(+) lymphoid cells. *Nature* 463: 540–544
- Nakayama K, Katoh Y (2018) Ciliary protein trafficking mediated by IFT and BBSome complexes with the aid of kinesin-2 and dynein-2 motors. *J Biochem* 163: 155–164
- Nie YC, Waite J, Brewer F, Sunshine MJ, Littman DR, Zou YR (2004) The role of CXCR4 in maintaining peripheral B cell compartments and humoral immunity. *J Exp Med* 200: 1145–1156
- Niederlova V, Modrak M, Tsyklauri O, Huranova M, Stepanek O (2019) Meta-analysis of genotype-phenotype associations in Bardet-Biedl



- syndrome uncovers differences among causative genes. *Hum Mutat* 40: 2068–2087
- Norrasethada L, Khumpoo W, Rattarittamrong E, Rattanathammethee T, Chai-Adisaksotha C, Tantiworawit A (2019) The use of mean platelet volume for distinguishing the causes of thrombocytopenia in adult patients. *Hematol Rep* 11: 23–27
- O'Dea D, Parfrey PS, Harnett JD, Hefferton D, Cramer BC, Green J (1996) The importance of renal impairment in the natural history of Bardet-Biedl syndrome. *Am J Kidney Dis* 27: 776–783
- Ohno T, Aune D, Heath AK (2020) Adiposity and the risk of rheumatoid arthritis: a systematic review and meta-analysis of cohort studies. *Sci Rep* 10: 16006
- Owczarczyk-Saczonek A, Placek W (2017) Compounds of psoriasis with obesity and overweight. *Postep Hig Med Dosw* 71: 761–772
- Palmer E, Drobek A, Stepanek O (2016) Opposing effects of actin signaling and LFA-1 on establishing the affinity threshold for inducing effector T-cell responses in mice. *Eur J Immunol* 46: 1887–1901
- Park HS, Park JY, Yu R (2005) Relationship of obesity and visceral adiposity with serum concentrations of CRP, TNF-alpha and IL-6. *Diabetes Res Clin Pr* 69: 29–35
- Paz G, Mastronardi C, Franco CB, Wang KB, Wong ML, Licinio J (2012) Leptin: molecular mechanisms, systemic pro-inflammatory effects, and clinical implications. *Arq Bras Endocrinol* 56: 597–607
- Plotnikova OV, Pugacheva EN, Golemis EA (2009) Primary cilia and the cell cycle. *Method Cell Biol* 94: 137–160
- Procaccini C, Jirillo E, Matarese G (2012) Leptin as an immunomodulator. *Mol Aspects Med* 33: 35–45
- Putoux A, Attie-Bitach T, Martinovic J, Gubler MC (2012) Phenotypic variability of Bardet-Biedl syndrome: focusing on the kidney. *Pediatr Nephrol* 27: 7–15
- Rahmouni K, Fath MA, Seo S, Thedens DR, Berry CJ, Weiss R, Nishimura DY, Sheffield VC (2008) Leptin resistance contributes to obesity and hypertension in mouse models of Bardet-Biedl syndrome. *J Clin Invest* 118: 1458–1467
- Ran FA, Hsu PD, Wright J, Agarwala V, Scott DA, Zhang F (2013) Genome engineering using the CRISPR-Cas9 system. *Nat Protoc* 8: 2281–2308
- Reis BS, Lee K, Fanok MH, Mascaraque C, Amoury M, Cohn LB, Rogoz A, Danner OS, Moraes-Vieira PM, Domingos AI et al (2015) Leptin receptor signaling in T cells is required for Th17 differentiation. *J Immunol* 194: 5253–5260
- Richter J, Traver D, Willert K (2017) The role of Wnt signaling in hematopoietic stem cell development. *Crit Rev Biochem Mol* 52: 414–424
- de la Roche M, Ritter AT, Angus KL, Dinsmore C, Earnshaw CH, Reiter JF, Griffiths GM (2013) Hedgehog signaling controls T cell killing at the immunological synapse. *Science* 342: 1247–1250
- de la Roche M, Asano Y, Griffiths GM (2016) Origins of the cytolytic synapse. *Nat Rev Immunol* 16: 421–432
- Ross AJ, May-Simera H, Eichers ER, Kai M, Hill J, Jagger DJ, Leitch CC, Chapple JP, Munro PM, Fisher S et al (2005) Disruption of Bardet-Biedl syndrome ciliary proteins perturbs planar cell polarity in vertebrates. *Nat Genet* 37: 1135–1140
- Rowbotham NJ, Furmanski AL, Hager-Theodorides AL, Ross SE, Drakopoulou E, Koufaris C, Outram SV, Crompton T (2008) Repression of hedgehog signal transduction in T-lineage cells increases TCR-induced activation and proliferation. *Cell Cycle* 7: 904–908
- Schmoeller D, Picarelli MM, Munhoz TP, de Figueiredo CEP, Staub HL (2017) Mean platelet volume and immature platelet fraction in autoimmune disorders. *Front Med-Lausanne* 4: 146
- Shah DK, Hager-Theodorides AL, Outram SV, Varas A, Crompton T (2004) Reduced thymocyte development in sonic hedgehog knockout embryos. *J Immunol* 172: 2296–2306
- Shimshek DR, Kim J, Hubner MR, Spergel DJ, Buchholz F, Casanova E, Stewart AF, Seeburg PH, Sprengel R (2002) Codon-improved Cre recombinase (iCre) expression in the mouse. *Genesis* 32: 19–26
- Sindhu S, Thomas R, Shihab P, Sriraman D, Behbehani K, Ahmad R (2015) Obesity is a positive modulator of IL-6R and IL-6 expression in the subcutaneous adipose tissue: significance for metabolic inflammation. *PLoS One* 10: e0133494
- Singh S, Dulai PS, Zarrinpar A, Ramamoorthy S, Sandborn WJ (2017) Obesity in IBD: epidemiology, pathogenesis, disease course and treatment outcomes. *Nat Rev Gastro Hepat* 14: 110–121
- Skarnes WC, Rosen B, West AP, Koutourakis M, Bushell W, Iyer V, Mujica AO, Thomas M, Harrow J, Cox T et al (2011) A conditional knockout resource for the genome-wide study of mouse gene function. *Nature* 474: 337–342
- Song RH, Wang B, Yao QM, Li Q, Jia X, Zhang JA (2019) The impact of obesity on thyroid autoimmunity and dysfunction: a systematic review and meta-analysis. *Front Immunol* 10: 2349
- Sonoda E, Pewznerjung Y, Schwers S, Taki S, Jung S, Eilat D, Rajewsky K (1997) B cell development under the condition of allelic inclusion. *Immunity* 6: 225–233
- Staal FJT, Chhatta A, Mikkers H (2016) Caught in a Wnt storm: complexities of Wnt signaling in hematopoiesis. *Exp Hematol* 44: 451–457
- Stasi R (2012) How to approach thrombocytopenia. *Hematol-Am Soc Hemat* 2012: 191–197
- Stephen LA, ElMaghloob Y, McIlwraith MJ, Yelland T, Sanchez PC, Roda-Navarro P, Ismail S (2018) The ciliary machinery is repurposed for T cell immune synapse trafficking of LCK. *Dev Cell* 47: 122–132.e4
- Stone MA, Mayberry JF, Baker R (2003) Prevalence and management of inflammatory bowel disease: a cross-sectional study from central England. *Eur J Gastroenterol Hepatol* 15: 1275–1280
- Sudlow C, Gallacher J, Allen N, Beral V, Burton P, Danesh J, Downey P, Elliott P, Green J, Landray M et al (2015) UK biobank: an open access resource for identifying the causes of a wide range of complex diseases of middle and old age. *PLoS Medicine* 12: e1001779
- Tamura M, Sato MM, Nashimoto M (2011) Regulation of CXCL12 expression by canonical Wnt signaling in bone marrow stromal cells. *Int J Biochem Cell Biol* 43: 760–767
- Tanaka S, Isoda F, Ishihara Y, Kimura M, Yamakawa T (2001) T lymphopenia in relation to body mass index and TNF-alpha in human obesity: adequate weight reduction can be corrective. *Clin Endocrinol* 54: 347–354
- Taylor PN, Albrecht D, Scholz A, Gutierrez-Buey G, Lazarus JH, Dayan CM, Okosieme OE (2018) Global epidemiology of hyperthyroidism and hypothyroidism. *Nat Rev Endocrinol* 14: 301–316
- Tschop J, Nogueiras R, Haas-Lockie S, Kasten KR, Castaneda TR, Huber N, Guanciale K, Perez-Tilve D, Habegger K, Ottaway N et al (2010) CNS leptin action modulates immune response and survival in sepsis. *J Neurosci* 30: 6036–6047
- Vaisse C, Reiter JF, Berbari NF (2017) Cilia and obesity. *Cold Spring Harbor Perspect Biol* 9: a028217
- Versini M, Jeandel PY, Rosenthal E, Shoenfeld Y (2014) Obesity in autoimmune diseases: not a passive bystander. *Autoimmun Rev* 13: 981–1000
- Visser M, Bouter LM, McQuillan GM, Wener MH, Harris TB (1999) Elevated C-reactive protein levels in overweight and obese adults. *JAMA* 282: 2131–2135
- Vivar OI, Masi G, Carpiere JM, Magalhaes JG, Galgano D, Pazour GJ, Amigorena S, Hivroz C, Baldari CT (2016) IFT20 controls LAT recruitment to the immune synapse and T-cell activation *in vivo*. *Proc Natl Acad Sci USA* 113: 386–391

- Wang TT, He CQ (2018) Pro-inflammatory cytokines: the link between obesity and osteoarthritis. *Cytokine Growth Factor Rev* 44: 38–50
- Wei Q, Zhang YX, Li YJ, Zhang Q, Ling K, Hu JH (2012) The BBSome controls IFT assembly and turnaround in cilia. *Nat Cell Biol* 14: 950–957
- Wheatley DN, Wang AM, Strugnell GE (1996) Expression of primary cilia in mammalian cells. *Cell Biol Int* 20: 73–81
- Williams CL, McIntyre JC, Norris SR, Jenkins PM, Zhang L, Pei QL, Verhey K, Martens JR (2014) Direct evidence for BBSome-associated intraflagellar transport reveals distinct properties of native mammalian cilia. *Nat Commun* 5: 5813
- Wormser O, Gradstein L, Yogev Y, Perez Y, Kadir R, Goliand I, Sadka Y, El Riati S, Flusser H, Nachmias D et al (2019) SCAPER localizes to primary cilia and its mutation affects cilia length, causing Bardet-Biedl syndrome. *Eur J Hum Genet* 27: 928–940
- Ye F, Nager AR, Nachury MV (2018) BBSome trains remove activated GPCRs from cilia by enabling passage through the transition zone. *J Cell Biol* 217: 1847–1868
- Yuan X, Garrett-Sinha LA, Sarkar D, Yang S (2014) Deletion of IFT20 in early stage T lymphocyte differentiation inhibits the development of collagen-induced arthritis. *Bone Res* 2: 14038
- Zehentmeier S, Pereira JP (2019) Cell circuits and niches controlling B cell development. *Immunol Rev* 289: 142–157
- Zhang QH, Nishimura D, Seo S, Vogel T, Morgan DA, Searby C, Bugge K, Stone EM, Rahmouni K, Sheffield VC (2011) Bardet-Biedl syndrome 3 (Bbs3) knockout mouse model reveals common BBS-associated phenotypes and Bbs3 unique phenotypes. *Proc Natl Acad Sci USA* 108: 20678–20683
- Zhang Q, Yu D, Seo S, Stone EM, Sheffield VC (2012a) Intrinsic protein-protein interaction-mediated and chaperonin-assisted sequential assembly of stable bardet-biedl syndrome protein complex, the BBSome. *J Biol Chem* 287: 20625–20635
- Zhang QH, Seo S, Bugge K, Stone EM, Sheffield VC (2012b) BBS proteins interact genetically with the IFT pathway to influence SHH-related phenotypes. *Hum Mol Genet* 21: 1945–1953